

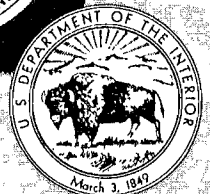
RI 9240

REPORT OF INVESTIGATIONS/1989

Performance of a Novel Bump Control Pillar Extracting Technique During Room-and-Pillar Retreat Coal Mining

By Alan A. Campoli, David C. Oyler, and Frank E. Chase

BUREAU OF MINES



UNITED STATES DEPARTMENT OF THE INTERIOR

Report of Investigations 9240

**Performance of a Novel Bump Control Pillar
Extracting Technique During Room-and-Pillar
Retreat Coal Mining**

By Alan A. Campoli, David C. Oyler, and Frank E. Chase

**UNITED STATES DEPARTMENT OF THE INTERIOR
Manuel J. Lujan, Jr., Secretary**

**BUREAU OF MINES
T S Ary, Director**

Library of Congress Cataloging in Publication Data:

Campoli, A. A. (Alan A.)

Performance of a novel bump control pillar extracting technique during room-and-pillar retreat coal mining.

(Report of investigations; 9240)

Bibliography: p. 38.

Supt. of Docs. no.: I 28.23:9240.

1. Pillaring (Mining). 2. Coal mines and mining—West Virginia—McDowell County. I. Oyler, David C. II. Chase, Frank E. III. Title. IV. Series: Report of investigations (United States. Bureau of Mines); 9240.

TN23.U43

[TN292]

622 s [622'.334]

88-600453

CONTENTS

Page

| | |
|---|----|
| Abstract | 1 |
| Introduction | 2 |
| Acknowledgments | 2 |
| Geologic setting | 2 |
| Background | 8 |
| Reaction of coal pillars to mining | 10 |
| Section-wide reaction by period | 11 |
| History of a typical coal pillar | 25 |
| Detailed convergence surveys during mining | 25 |
| Reaction of associated strata to mining | 29 |
| In situ horizontal roof stress | 29 |
| Relative mining-induced pressure changes in the roof | 29 |
| Mining-induced associated strata movement | 30 |
| Localized destressing techniques | 30 |
| Shot firing | 31 |
| Auger drilling | 32 |
| Summary and conclusions | 36 |
| References | 37 |
| Appendix.—Borehole deformation gauge procedures and results | 38 |

ILLUSTRATIONS

| | |
|---|----|
| 1. Generalized stratigraphic column for Olga Mine | 2 |
| 2. Structure contour map on base of Pocahontas No. 4 Coalbed | 3 |
| 3. Overburden map for Pocahontas No. 4 Coalbed | 4 |
| 4. Sandstone floor thickness and bump correlation map | 6 |
| 5. Sandstone roof thickness and bump correlation map | 7 |
| 6. Map of 9 Right study area, September 1985 | 8 |
| 7. Map of 9 Right study area, June 1986 | 9 |
| 8. Generalized pillar splitting extraction sequence | 9 |
| 9. Isopach map of pressure changes from February 23 through March 22, 1986 | 10 |
| 10. Isopach map of roof-to-floor convergence from February 23 through March 22, 1986 | 11 |
| 11. Isopach map of pressure changes from March 23 through April 19, 1986 | 12 |
| 12. Isopach map of roof-to-floor convergence from March 23 through April 19, 1986 | 13 |
| 13. Isopach map of pressure changes from April 20 through May 17, 1986 | 14 |
| 14. Isopach map of roof-to-floor convergence from April 20 through May 17, 1986 | 15 |
| 15. Dilation of chain pillars instrumented with extensometers from April 20 through May 17, 1986 | 16 |
| 16. Isopach map of pressure changes from May 18 through June 14, 1986 | 16 |
| 17. Isopach map of roof-to-floor convergence from May 18 through June 14, 1986 | 17 |
| 18. Dilation of chain pillars instrumented with extensometers from May 18 through June 14, 1986 | 17 |
| 19. Isopach map of pressure changes from June 15 through July 12, 1986 | 18 |
| 20. Isopach map of roof-to-floor convergence from June 15 through July 12, 1986 | 19 |
| 21. Dilation of chain pillars instrumented with extensometers from June 15 through July 12, 1986 | 19 |
| 22. Isopach map of pressure changes from July 13 through August 9, 1986 | 20 |
| 23. Isopach map of roof-to-floor convergence from July 13 through August 9, 1986 | 21 |
| 24. Dilation of chain pillars instrumented with extensometers from July 13 through August 9, 1986 | 21 |
| 25. Isopach map of roof-to-floor convergence from August 10 through September 6, 1986 | 22 |
| 26. Dilation of chain pillars instrumented with extensometers from August 10 through September 6, 1986 .. | 22 |
| 27. Isopach map of roof-to-floor convergence from September 7 through September 27, 1986 | 23 |
| 28. Dilation of chain pillars instrumented with extensometers from September 7 through September 27, 1986 | 23 |
| 29. Coal cell pressure in and roof-to-floor convergence around a typical instrumented chain pillar, from November 1, 1985 to September 4, 1986 | 24 |
| 30. Map of detailed roof-to-floor convergence surveys | 26 |
| 31. Detailed roof-to-floor convergence versus cut type | 27 |
| 32. Illustration of location sensitivity of wing cut detailed roof-to-floor convergence surveys | 27 |

ILLUSTRATIONS—Continued

Page

| | |
|---|----|
| 33. Barrier split cut detailed roof-to-floor convergence surveys in area of lost-time, barrier-splitting bump accident | 28 |
| 34. Hollow inclusion cell principal stress data, from February 25 to October 2, 1986 | 30 |
| 35. Shot fire roof-to-floor convergence survey locations and hole configurations | 31 |
| 36. Roof-to-floor convergence versus time for shot fire surveys 1, 2, and 3 | 32 |
| 37. Auger drilling survey location map | 33 |
| 38. Total roof-to-floor convergence versus total cuttings volume produced for 11 auger drilling surveys | 33 |
| 39. Plan view of auger drilling survey 1 | 34 |
| 40. Plan view of auger drilling surveys 9 and 10 | 34 |
| 41. Cumulative cuttings volume and cumulative roof-to-floor convergence versus drilling depth for auger drilling surveys 9 and 10 | 34 |
| 42. Roof-to-floor convergence versus cuttings volume produced per steel advance | 35 |
| 43. Illustration of effect of auger drilling in high-stress pillars | 35 |
| 44. Plan view of auger drilling survey 4 | 35 |
| 45. Plan view of auger drilling survey 5 | 35 |
| 46. Plan view of auger drilling survey 6 | 36 |

TABLES

| | |
|---|----|
| 1. Physical properties of rock in 9 Right section of Olga Mine | 5 |
| A-1. Anisotropic and isotropic stress computation of borehole deformation gauge results | 38 |

UNIT OF MEASURE ABBREVIATIONS USED IN THIS REPORT

| | | | |
|----------------------|---------------------------|------|--------------------------------------|
| cal/g | calorie per gram | h | hour |
| ft | foot | in | inch |
| ft · lbf | foot-pound (force) | lbf | pound (force) |
| ft/s | foot per second | pct | percent |
| ft ³ /min | cubic foot per minute | psi | pound (force) per square inch |
| g | gram | psig | pound (force) per square inch, gauge |
| g/cm ³ | gram per cubic centimeter | rpm | revolution per minute |
| gal | gallon | st | short ton |

PERFORMANCE OF A NOVEL BUMP CONTROL PILLAR EXTRACTING TECHNIQUE DURING ROOM-AND-PILLAR RETREAT COAL MINING

By Alan A. Campoli,¹ David C. Oyler,²
and Frank E. Chase³

ABSTRACT

Retreat pillar mining concentrates stresses on workings directly outby gob areas, which can result in coal mine bumps. The development of bump-control design criteria by the U.S. Bureau of Mines was furthered by data from a novel bump control mining method at the Olga Mine, McDowell County, WV. The pillar splitting, retreat mining system induced large pillar pressure increases and roof-to-floor convergence. Roof-to-floor convergence monitoring proved to be a valuable tool in evaluating the pillar splitting mining method and localized destressing techniques. Maximum strain energy storage in chain pillars appears to have occurred just prior to the first of four split cuts. At that point a 15-ft-wide, highly fractured perimeter confined the core of the 55- by 70-ft pillars, permitting the pillar core to support tremendous pressures. Splitting the chain pillars into two 17.5- by 70-ft wings removed the confinement load, resulting in pillar yield. Thus, the pillar splitting mining method successfully redistributed the weight of the roof away from the pillar line. Shot fire and auger drilling destressing techniques augmented the pillar splitting mining method by redistributing the weight of the roof.

¹Mining engineer.

²Mechanical engineer.

³Geologist.

Pittsburgh Research Center, U.S. Bureau of Mines, Pittsburgh, PA.

INTRODUCTION

Retreat room-and-pillar coal mining concentrates stress in the pillars adjacent to expanding gob areas. When mining is conducted at great depth and between unyielding roof and floor, violent coal pillar failure or bumps may result. These bumps vary from minor vibrations without significant strata movement, to thousands of tons of coal ejected into mine workings.

Coal mine bumps have resulted in 14 fatalities from 1959 through 1986, in Kentucky, West Virginia, and Pennsylvania. Prior investigations on coal mine bumps have

been documented by the Bureau (1)⁴ and other researchers (2-3). To obtain data for a better understanding of the bump phenomena, current Bureau research is employing a two-pronged effort of microseismic monitoring and detailed geologic and rock mechanics techniques (4). Both technologies were used to study bumps during retreat room-and-pillar mining at the Olga Mine, McDowell County, WV. The microseismic study (5) was completed just prior to the detailed geologic and rock mechanics study presented in this report.

ACKNOWLEDGMENTS

This work could not have been accomplished without the help of many people well acquainted with the coal mine bump phenomena. Martin Valeri, general superintendent, Chandra Sharma, mining engineer, Dwight Strong, superintendent, and Don Winstone, chief mining

engineer of Olga Mining Co.; and Dan Ashcraft, director of coal mines, and K. V. Rao, chief mining engineer of LTV, Inc., provided valued in-mine assistance, information, insight, and advice.

GEOLOGIC SETTING

Past mining experience suggests that bumps generally occur in areas where certain geologic conditions are met. Some of these conditions are excessive overburden, stiff roof and floor members, and widely spaced fracture patterns (1, 6). To determine if geologic conditions could be used to help anticipate bumps, the geology of previous bump locations at the Olga Mine was examined.

The Olga Mine extracts the Pocahontas No. 4 Coalbed (fig. 1). In the 9 Right section study area the coalbed thickness averages 66 in. The Pocahontas No. 4 Coalbed is a friable coal with a mean compressive strength of 2,400 psi, as indicated in table 1 (7). The coalbed dips northwest as shown in figure 2. The 9 Right section is located under the greatest overburden found on the property (fig. 3). Overburden ranges from 990 to slightly over 1,600 ft in the study area, and from approximately 400 to greater than 1,600 ft mine wide. Major bump sites occurred under overburden greater than 500 ft.

The Upper Pocahontas Sandstone is below the coalbed. This sandstone unit is laterally discontinuous in the interval 0 to 5 ft below the coalbed (fig. 1) (8). Within this 5-ft interval, the fine- to medium-grained Upper Pocahontas Sandstone sometimes laterally grades into a competent siltstone and into shale units. Physical property data for the roof, coal, and floor members are listed in table 1.

⁴Italic numbers in parentheses refer to items in the list of references preceding the appendix at the end of this report.

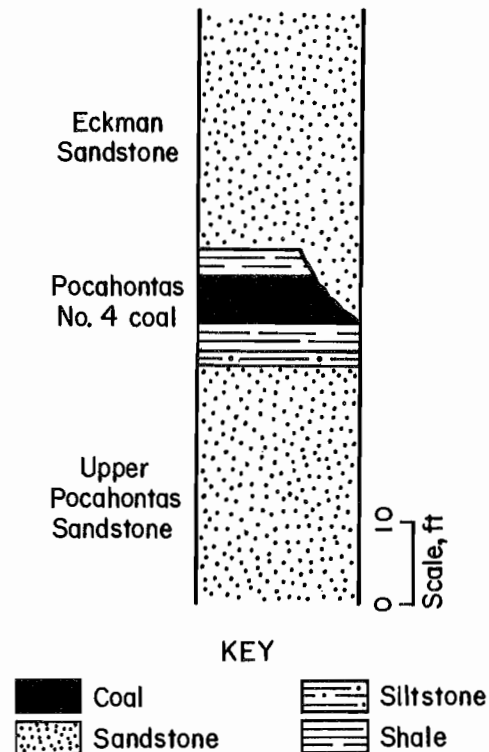


Figure 1.—Generalized stratigraphic column for Olga Mine.

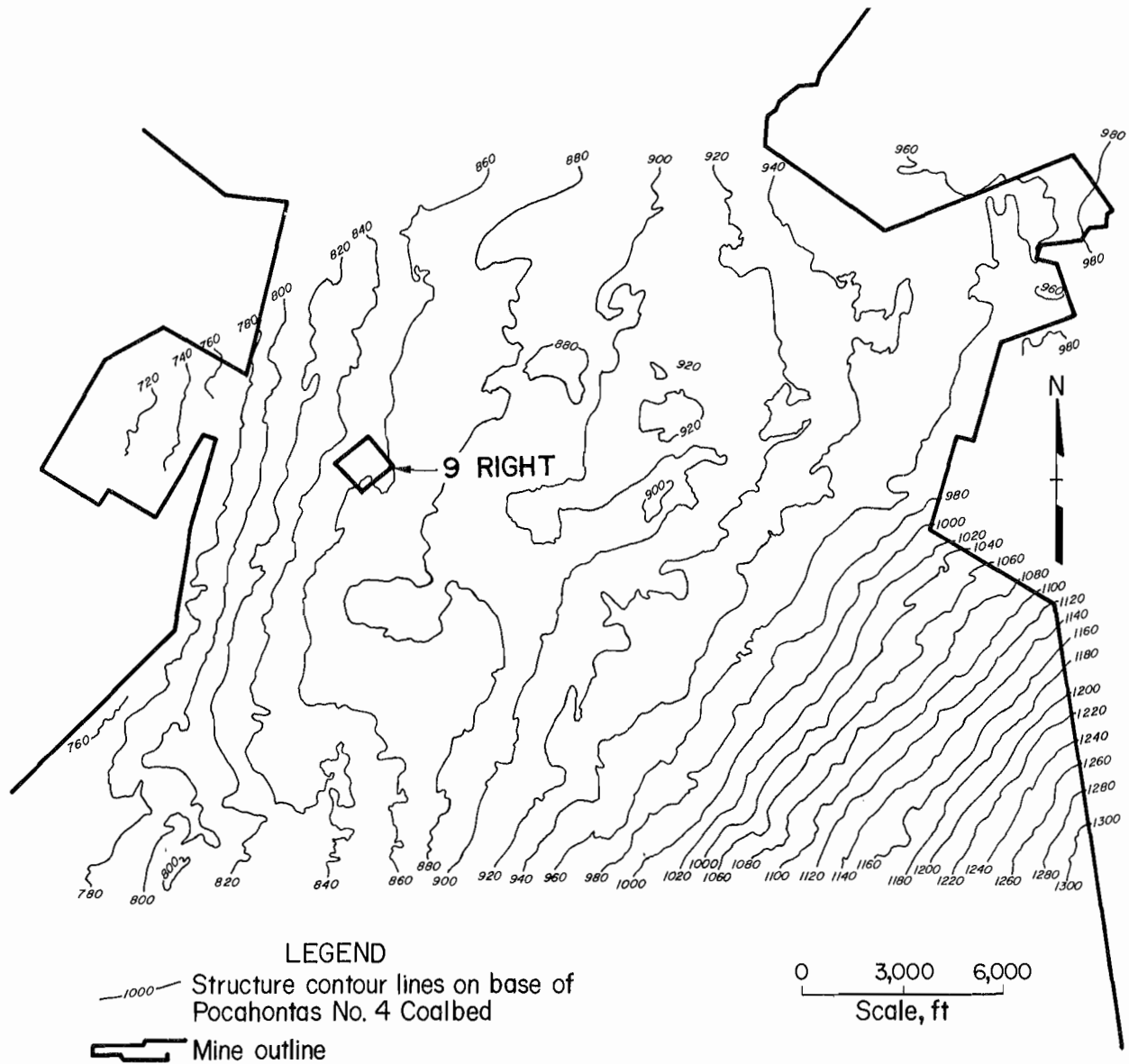


Figure 2.—Structure contour map on base of Pocahontas No. 4 Coalbed.

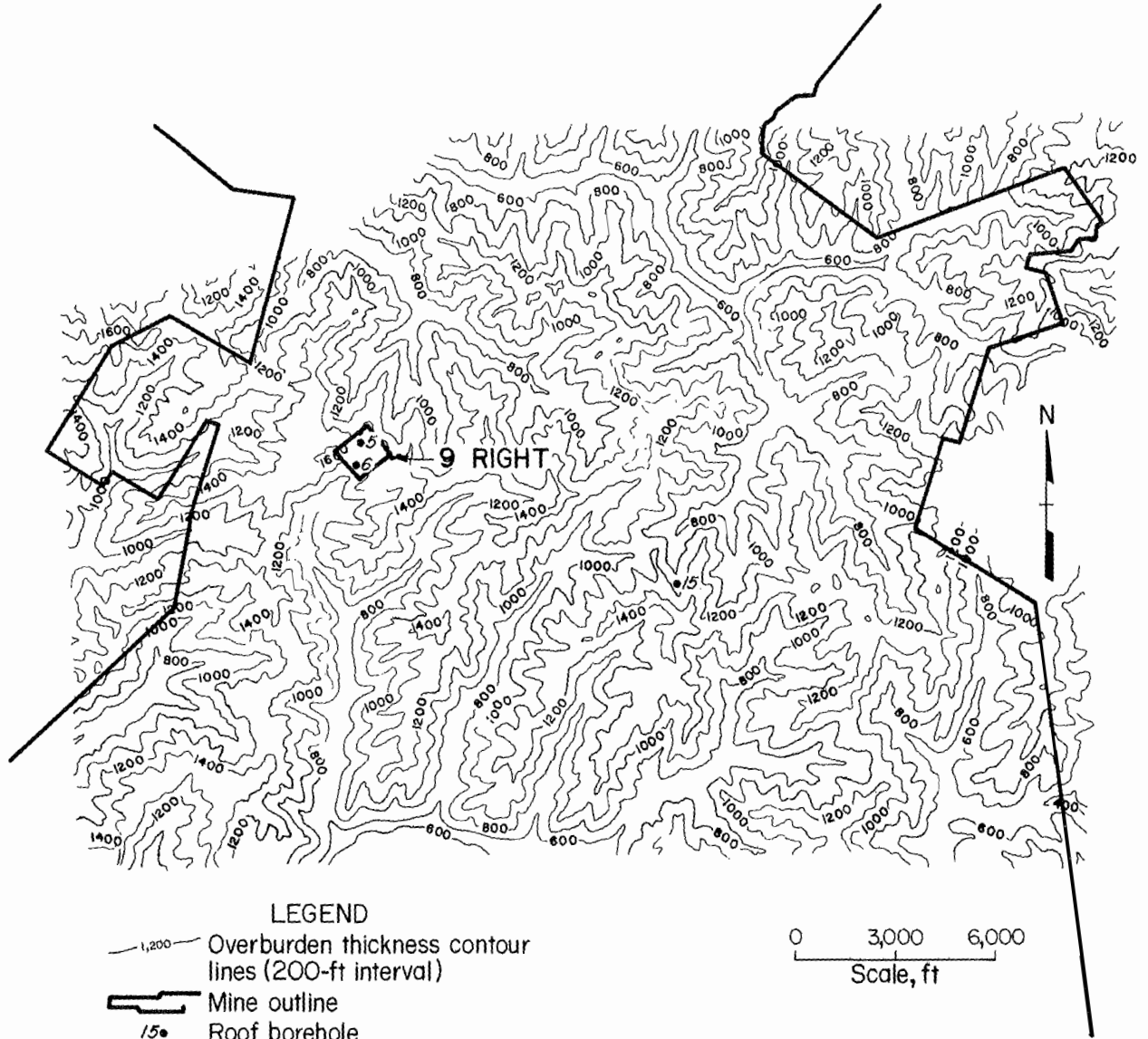


Figure 3.—Overburden map for Pocahontas No. 4 Coalbed.

Table 1.—Physical properties of rock in 9 Right section of Olga Mine

| Strata type | Mean | Standard deviation | Samples tested |
|---|--------|--------------------|----------------|
| Sandstone roof: | | | |
| Compressive strength psi .. | 24,200 | 1,900 | 40 |
| Tensile strength psi .. | 1,070 | 280 | 21 |
| Young's modulus ¹ 10 ⁶ psi .. | 5.16 | 0.04 | 3 |
| Poisson's ratio ¹ | 0.30 | 0.02 | 3 |
| Sandstone floor: | | | |
| Compressive strength psi .. | 21,900 | 2,700 | 15 |
| Tensile strength psi .. | 1,010 | 260 | 12 |
| Young's modulus ¹ 10 ⁶ psi .. | 5.45 | 0.39 | 3 |
| Poisson's ratio ¹ | 0.39 | 0.15 | 3 |
| Shale floor: | | | |
| Compressive strength psi .. | 12,600 | 2,600 | 18 |
| Tensile strength psi .. | 970 | 390 | 6 |
| Young's modulus ¹ 10 ⁶ psi .. | 3.97 | 0.83 | 3 |
| Poisson's ratio ¹ | 0.29 | 0.03 | 3 |
| Siltstone floor: | | | |
| Compressive strength psi .. | 16,900 | 3,400 | 14 |
| Tensile strength psi .. | 1,320 | 320 | 2 |
| Young's modulus ¹ 10 ⁶ psi .. | ND | ND | NAp |
| Poisson's ratio ¹ | ND | ND | NAp |
| Coal: | | | |
| Compressive strength psi .. | 2,400 | 500 | 6 |
| Tensile strength psi .. | ND | ND | NAp |
| Young's modulus ¹ psi .. | 0.61 | 0.17 | 6 |
| Poisson's ratio ¹ | 0.31 | 0.03 | 6 |

NAp Not applicable. ND Not determined.

¹Tangent (calculated at 50 pct of ultimate strength).

In addition to being strong relative to other coal measure rocks found in the eastern United States, the Upper Pocahontas Sandstone in the study area has a high rock quality designation (RQD) value of 95 to 100 pct (9). The siltstone found in the floor has an RQD of 90 pct and the shales 64 pct, with fractures mainly on bedding planes. All RQD data must be considered in the light of the fact that the entries tested were standing for over 50 years. The Upper Pocahontas Sandstone ranges in thickness from 50 to 75 ft (8). Under portions of the mine, this sandstone provides a competent and massive floor that does not heave or break readily (fig. 4). As figure 4 illustrates, bump areas associated with injuries or fatalities occurred primarily where the immediate and main floor were 80 to

100 pct sandstone. Eleven out of thirteen bumps associated with injuries or fatalities occurred in these areas.

The Eckman Sandstone forms the immediate and main roof at Olga and is a very stiff and massive unit (table 1). This unit can be 60 ft or more thick and contains a joint system that is unidirectional, extremely pronounced, and widely spaced. The roof has an RQD of 95 pct and a final rock mass rating (RMR) of 108 (10). As shown in figure 5, every bump occurred where the roof was predominantly sandstone (80-100 pct). Therefore, bump-prone areas may be anticipated based on these geologic correlations. Any area in the mine where the roof and floor members are predominantly composed of a stiff sandstone should be considered bump prone.

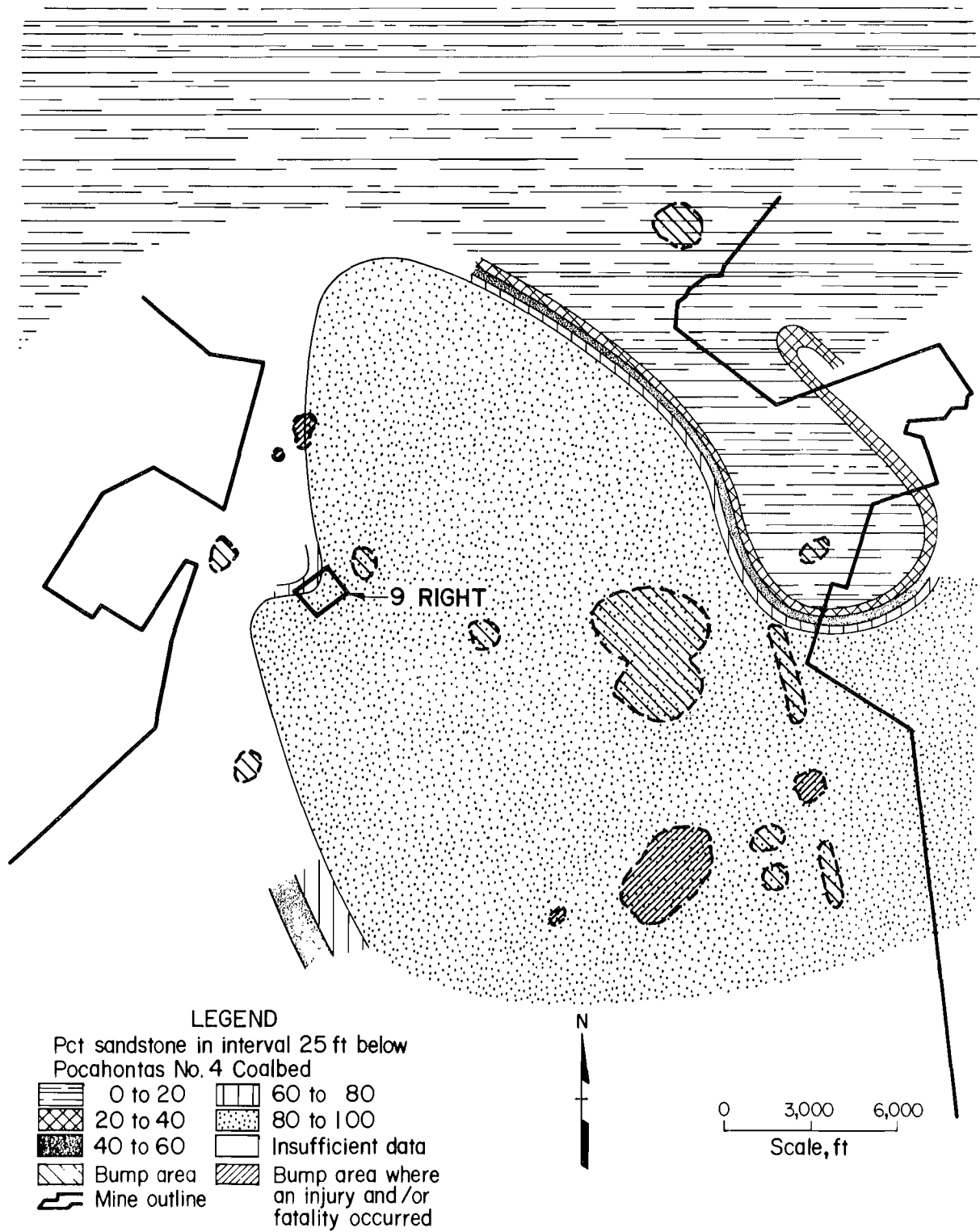


Figure 4.—Sandstone floor thickness and bump correlation map.

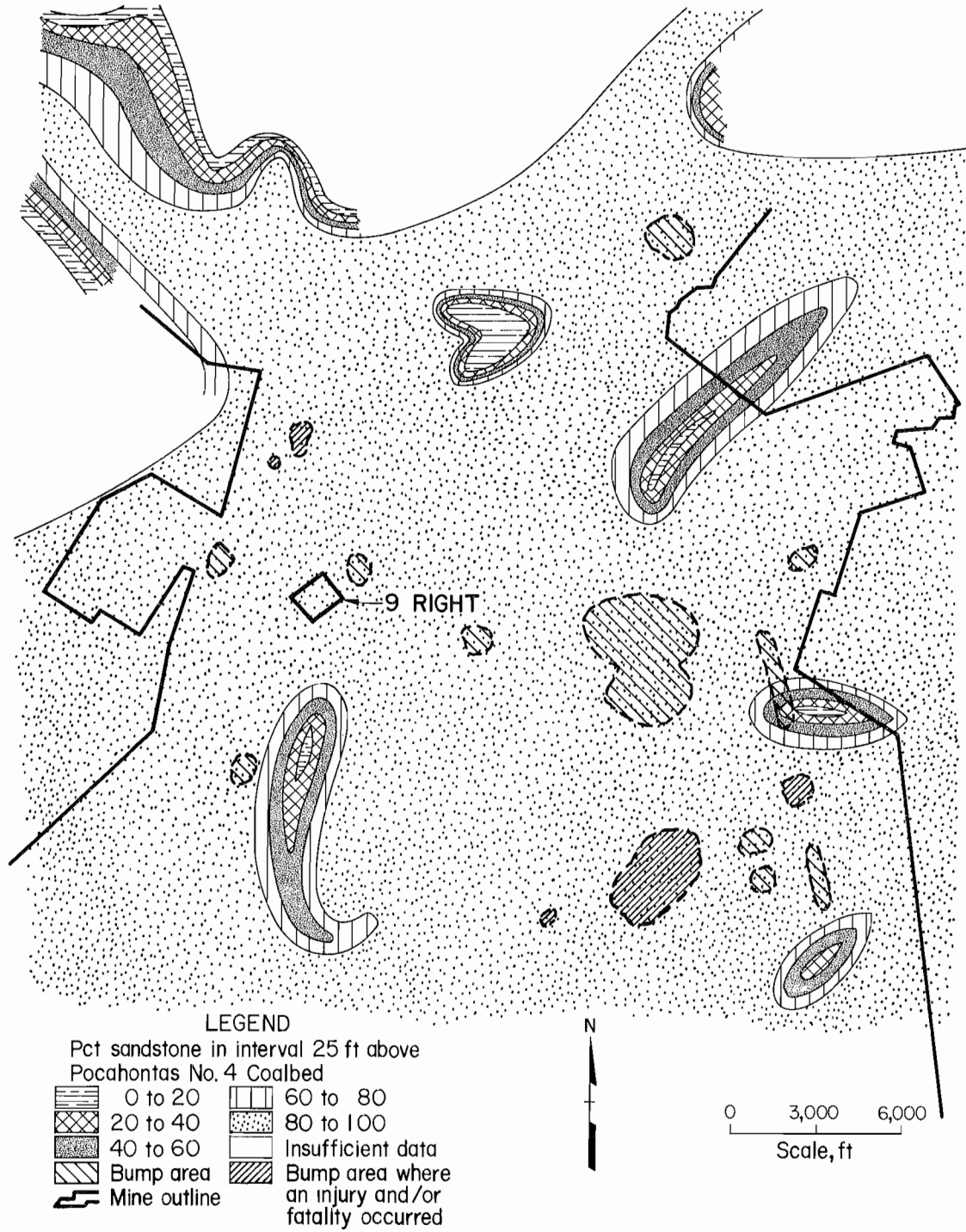


Figure 5.—Sandstone roof thickness and bump correlation map.

BACKGROUND

The Olga Mine was closed in early 1987. Prior to closure, the mine had been in continuous operation since the early 1900's. At the time of this study, mining was conducted exclusively by room-and-pillar methods using continuous miners. The majority of pillar retreat mining involved removing barrier pillars that had been left to protect access roadways driven many years ago. Often these barrier pillars were adjacent to gob areas. On October 18, 1983, two miners were killed by a bump on a continuous miner section in which such a barrier pillar was being extracted, under 1,100 ft of overburden (11). The 9 Right section was chosen for this study because it contained barrier pillars (pillars A through G on figure 6), which were in the same size and shape as the pillars (350 by 160 ft) involved in the 1983 fatalities.

Coal pillars exposed to high abutment pressures will yield or support the load, depending on their size and strength. A bump hazard may develop in a pillar of intermediate size, especially when it is surrounded by smaller yielding pillars (6). The intermediate-sized pillar in the

Pocahontas No. 4 Coalbed is generally less than 160 ft square and greater than 45 ft square (12). A pillar of this size will yield around its periphery. The yielded coal around the perimeter, along with the roof and floor, confine the pillar core. The lateral forces exerted by the pressurized core are counterbalanced by the lateral confinement provided by the yielded perimeter (6). The barrier pillars in the 9 Right section were mined through the intermediate-size range during the study.

The configuration of the study area at the onset of the investigation is diagramed in figure 6. Room-and-pillar retreat mining was underway in the area of 55- by 70-ft chain pillars shown in the left portion of the study area. Upon completion of the room-and-pillar retreat mining in the left portion, barrier splitting began in the main study area. The mining of the study area eventually resulted in the complete extraction of barrier pillars B, D, and F and the partial extraction of barrier pillars A, C, E, and G (fig. 6).

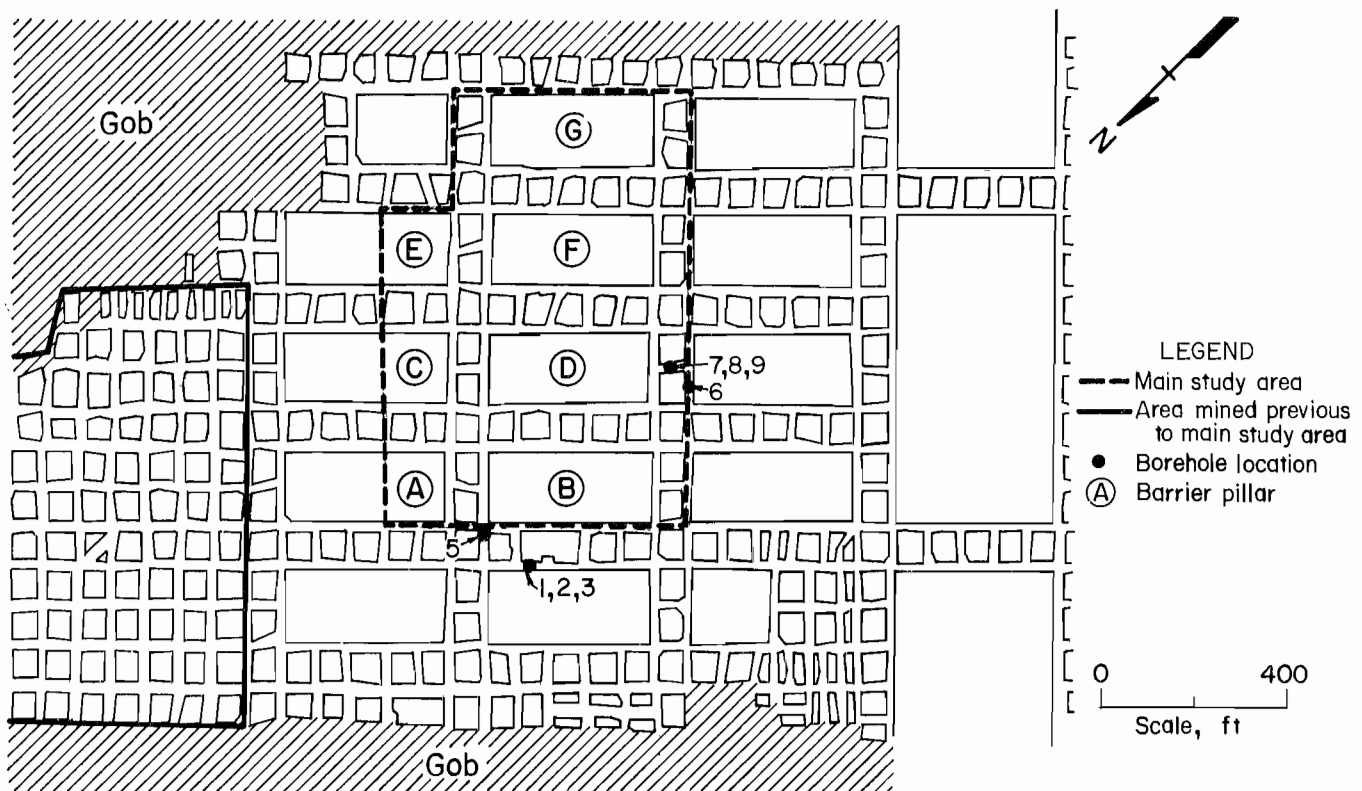


Figure 6.—Map of 9 Right study area, September 1985.

Barrier pillars B, D, and F were each completely split into ten 55- by 70-ft chain pillars by advance mining. Barrier pillars A, C, and E were each partially split into four chain pillars on the right and a 200- by 160-ft barrier on the left. These 200- by 160-ft barriers shield the new barrier pillar extraction section from the abutment zone pressure originating from the gob formed by the room-and-pillar retreat mining of the left portion, completed in January 1986. Advance mining was discontinued when high-stress areas were encountered during the splitting of the barrier pillar G (fig. 7). Abutment loads from an old gob area, inby barrier pillar G, caused excessive strain energy to be stored in the rigid barrier, which resulted in a bump that caused a lost-time injury. A nine by nine block of chain pillars, including most of barrier pillars A through F, was outlined when the retreat mining of the chain pillars began (fig. 7).

A novel pillar splitting method was the primary bump control technique used in extracting the 55- by 70-ft chain pillars in the outlined block. Three rows of pillars outby the gob were mined simultaneously to reduce strain energy storage. Generally the first two rows of pillars outby the gob were split down their long axes, leaving two 17.5- by 70-ft wings that yielded under abutment zone loading. The

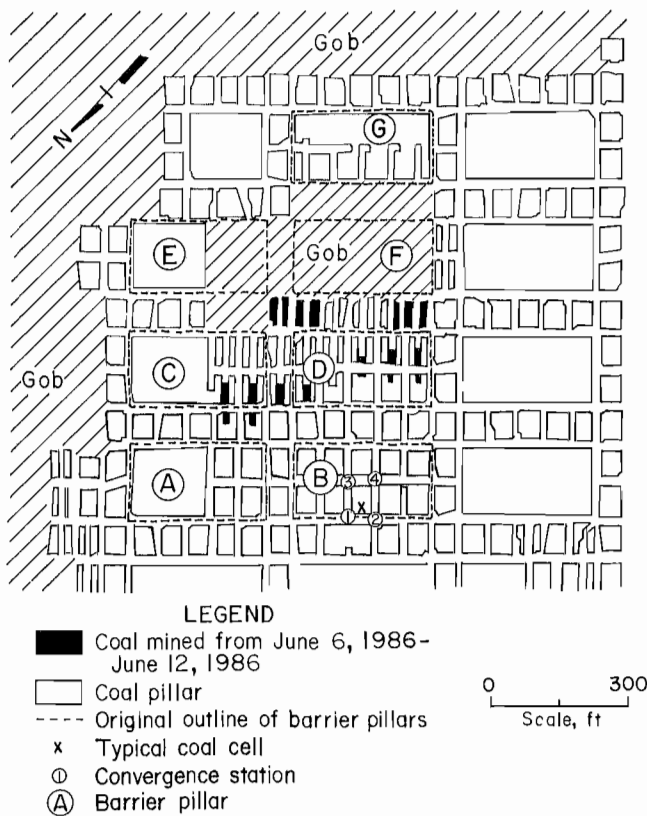


Figure 7.—Map of 9 Right study area, June 1986.

splitting of the third row was also generally begun prior to the removal of the wings adjacent to the gob. An example of this technique is the mining from June 6 through June 12, 1986 (fig. 7).

Figure 8 depicts the cut sequence on three rows of chain pillars. Only the cuts taken from a three by three block of pillars are numbered. Cuts from the inby pillars in the area labeled gob would be in the sequence, as would cuts in the adjacent pillars. Both were not labeled for the sake of clarity. The ability of the chain pillars to store strain energy and thus bump is destroyed by the time the third center splitting cut is completed. For example the pillars in row 2 will not bump after cuts 22, 23, and 24 are extracted.

Auger drilling and shot firing were applied to enhance the effectiveness of the pillar splitting mining method in controlling bumps. These localized stress reduction techniques were sometimes used to soften advance barrier and chain pillar retreat split cuts immediately prior to mining at various locations throughout the 9 Right section.

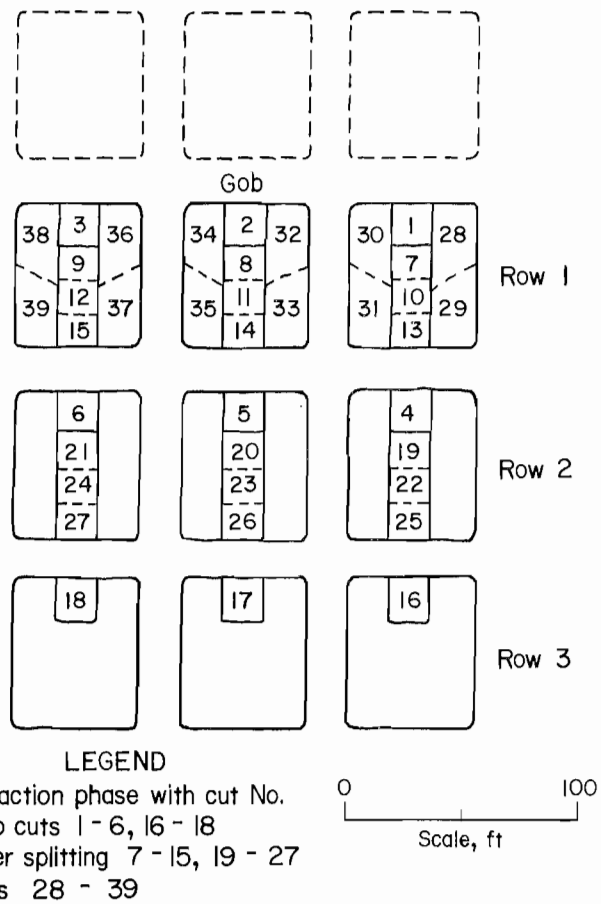


Figure 8.—Generalized pillar splitting extraction sequence.

REACTION OF COAL PILLARS TO MINING⁵

The reaction of the coal pillars to the barrier pillar mining in the study area was evaluated through measurement of change in vertical pressures within the pillars, roof-to-floor convergence in adjacent rooms, and dilation of the pillars upon yielding. Measurement of the pressure redistribution within coal pillars was accomplished with hydraulic coal cells, made from a copper flatjack and two aluminum platens (13). The cells were placed in coal pillars at depths of 15 and 30 ft. These oil-filled bladders were oriented to measure relative pressure changes in the vertical direction. All the cells were initially set at 2,500 psig, this value being the estimated average pressure over the barrier pillars prior to advance mining, calculated from the tributary theory (14).

Entry height was periodically measured with a portable, telescopic, tube extensometer capable of ± 0.001 -in accuracy over a 3- to 7-ft range. Permanent anchors were installed in the roof and floor at each roof-to-floor convergence station location. The extensometer was moved from station to station. The frequency of readings varied from biweekly to daily depending on the proximity of mining.

Dilation of coal pillars upon yielding was evaluated with multipoint extensometers. The wire extensometers were grouted into horizontal drill holes in the coal pillars at midseam height. Ten measurement point anchors were spaced 3 ft apart in each drill hole, over the extensometer's 30-ft length.

⁵Field data were collected by F. VanDyke, mining engineering technician, Pittsburgh Research Center.

SECTION-WIDE REACTION BY PERIOD

Mining activity in the main study area was divided into eight mining periods, approximately 4 weeks long each, to facilitate analysis. Barrier splitting advance mining comprised the first two periods and pillar extraction was addressed in the following five periods. Roof-to-floor convergence data were taken during all eight periods. Pillar dilation information was collected for the final six periods. Coal cell results are pertinent only for the first six periods, because the copper bladders failed at pressures from 10,000 to 13,000 psig. Coalbed vertical pressure often exceeded this value immediately prior to the first chain pillar split cut in the instrumented pillars. All three data sets are presented as changes from the beginning to end of each period. No cumulative effects are presented. The pillar pressure and convergence data are presented as contour overlays. This provides for the viewing of the data in an efficient manner. However, this does not allow for viewing of pressure changes that went up, then down during an individual period.

February 23 Through March 22, 1986

The barrier splitting advance mining of barrier pillars A, B, C, and D, conducted from February 23 through March 22, 1986, induced a maximum coal cell pressure increase of 4,550 psig (fig. 9). Roof-to-floor convergence readings over the same period displayed a maximum of 1.918 in (fig. 10).

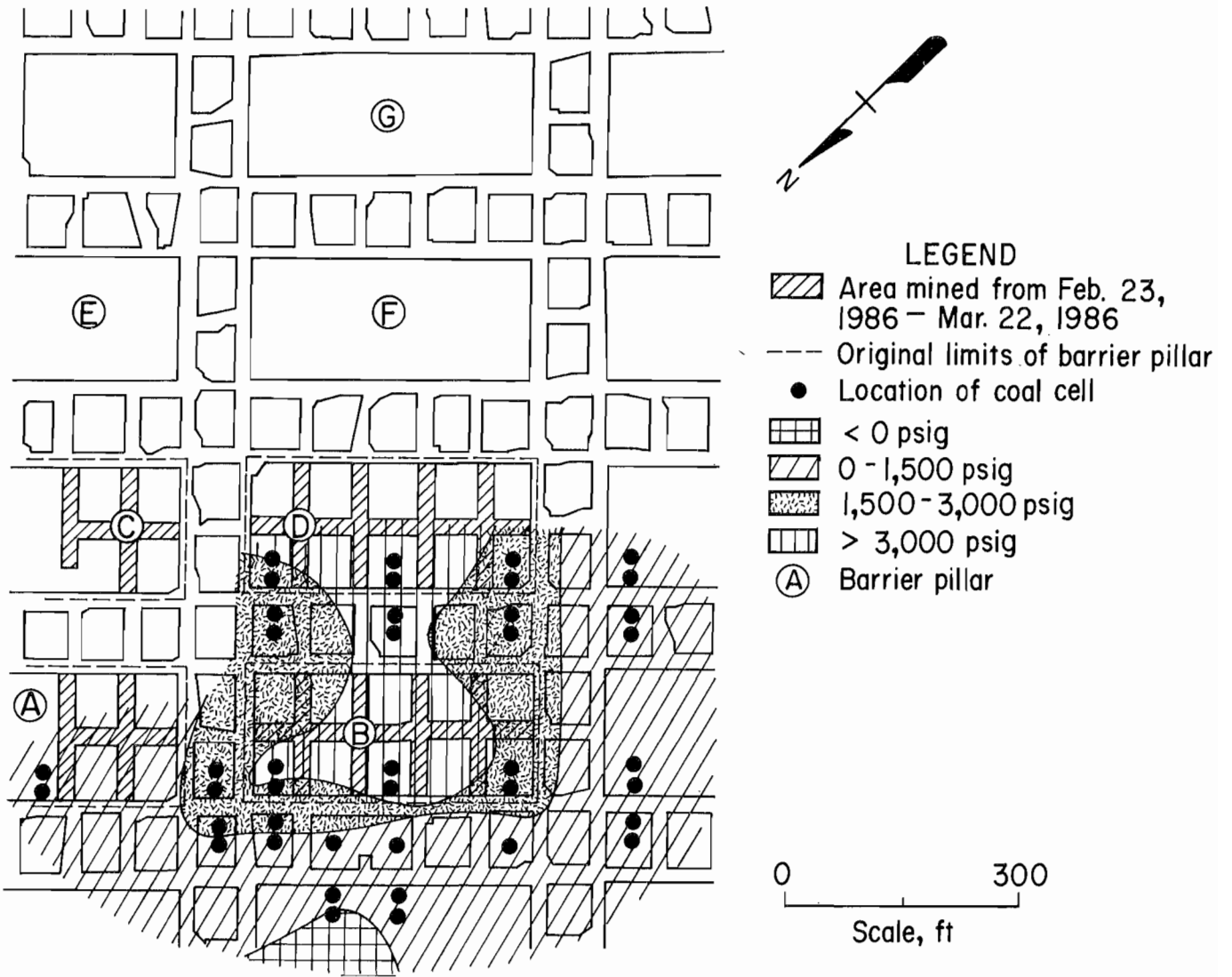


Figure 9.—Isopach map of pressure changes from February 23 through March 22, 1986.

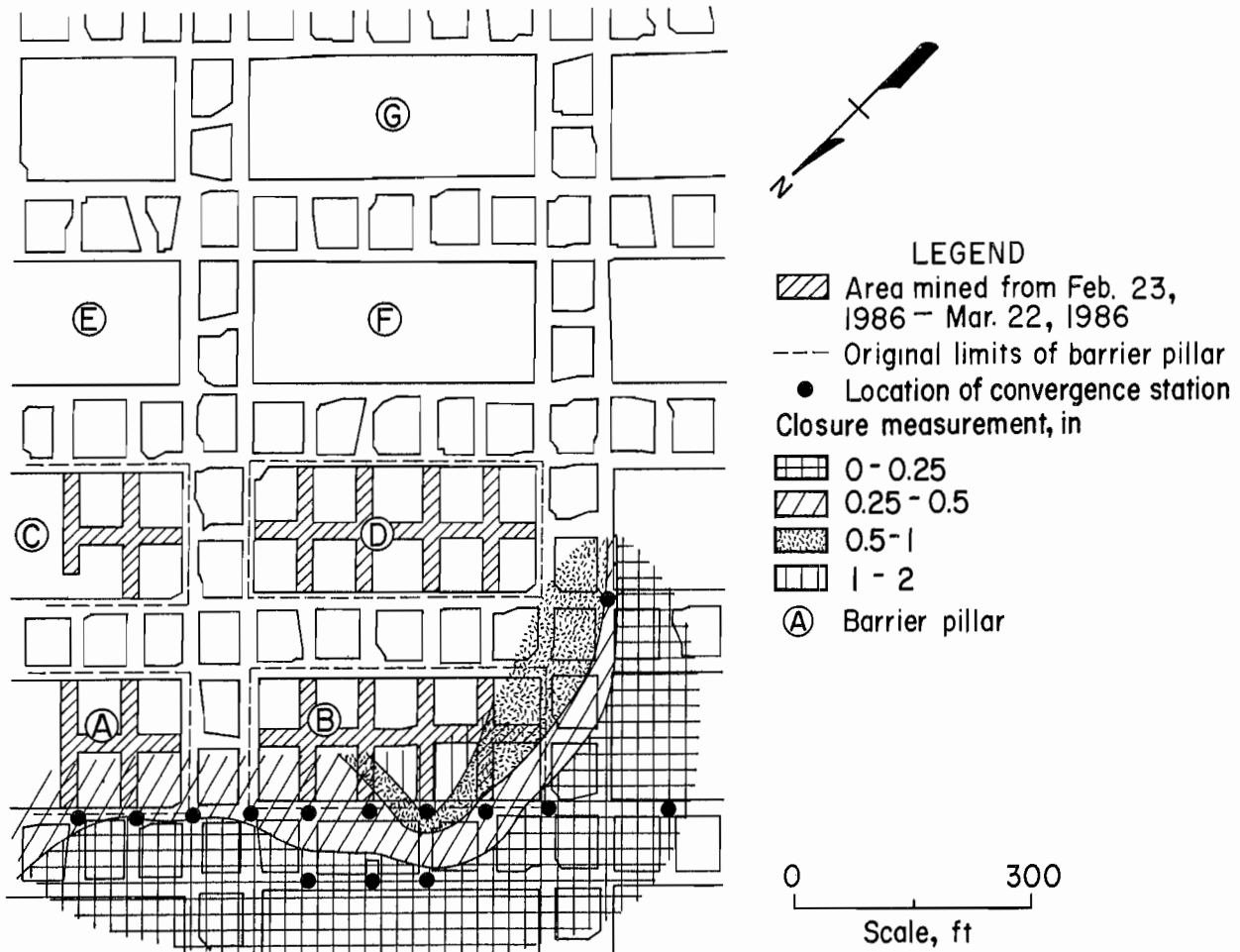


Figure 10.—Isopach map of roof-to-floor convergence from February 23 through March 22, 1986.

March 23 Through April 19, 1986

Barrier pillars E, F, and G were split into chain pillars in the 4 weeks from March 23 through April 19. No coal cell pressure increases over 1,500 psig were incurred (fig. 11). The maximum roof-to-floor convergence measured over this timeframe was 1.007 in (fig. 12). Negative coal cell pressure changes occurred in two pillars; roof-to-floor

convergence was at its maximum (>1 in) in the same area (figs. 11-12). The three cells all displayed peak loads of greater than 10,000 psi during the period. This is the first indication of what is theorized to be coal cell failure. Discounting this anomalous loading area, maximum changes were concentrated in the barrier pillars being split and their adjacent chain pillars.

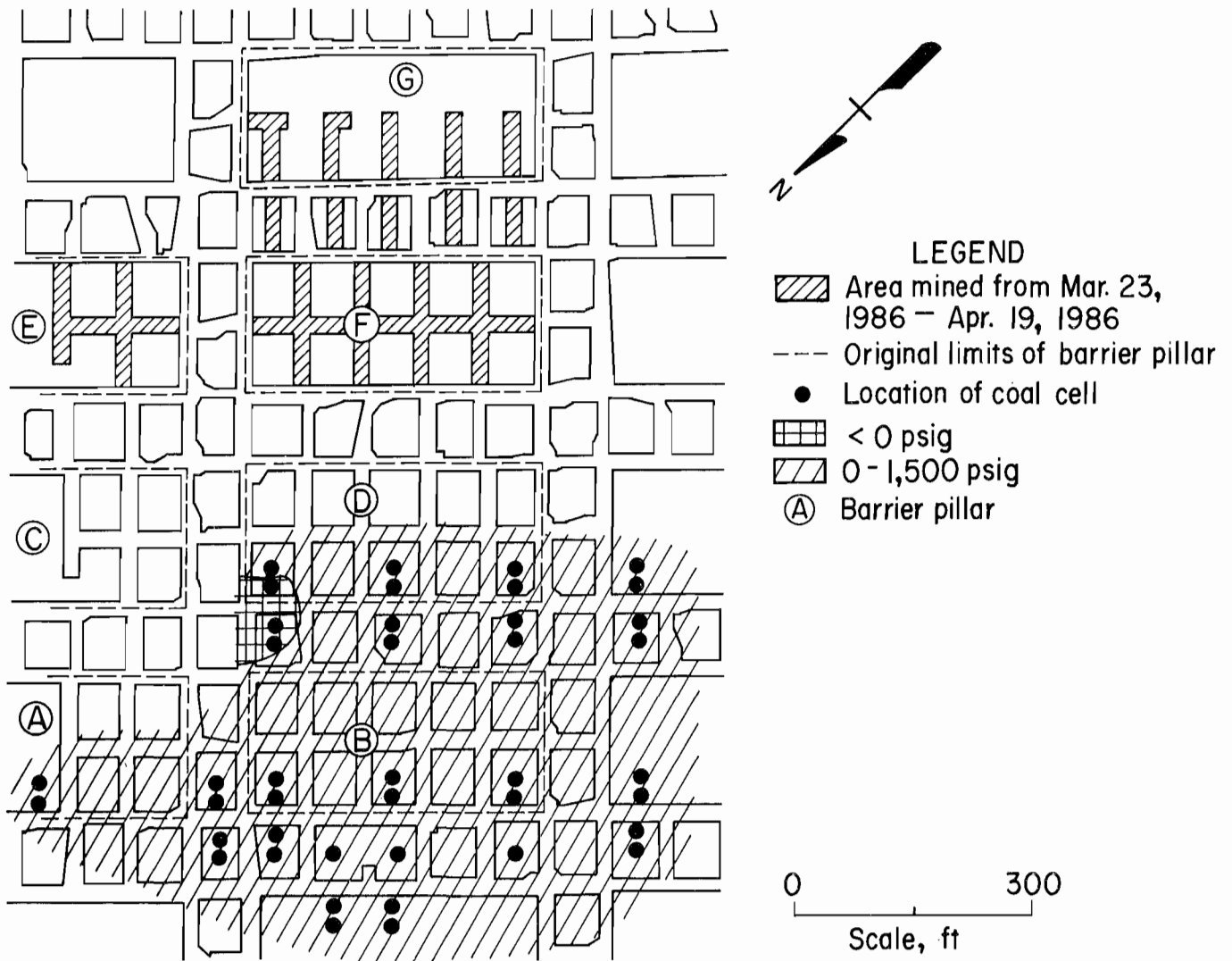


Figure 11.—Isopach map of pressure changes from March 23 through April 19, 1986.

April 20 Through May 17, 1987

Barrier splitting was discontinued and room-and-pillar retreat by the pillar splitting method was initiated in the period from April 20 through May 17. Barrier pillar G

proved to be highly stressed by abutment zone loads from an inby old gob area and from the recently created gob to northeast of the main study area (fig. 7). A lost-time injury resulted from a bump that occurred during the last cut attempted in barrier pillar G (fig. 13). Chain pillar

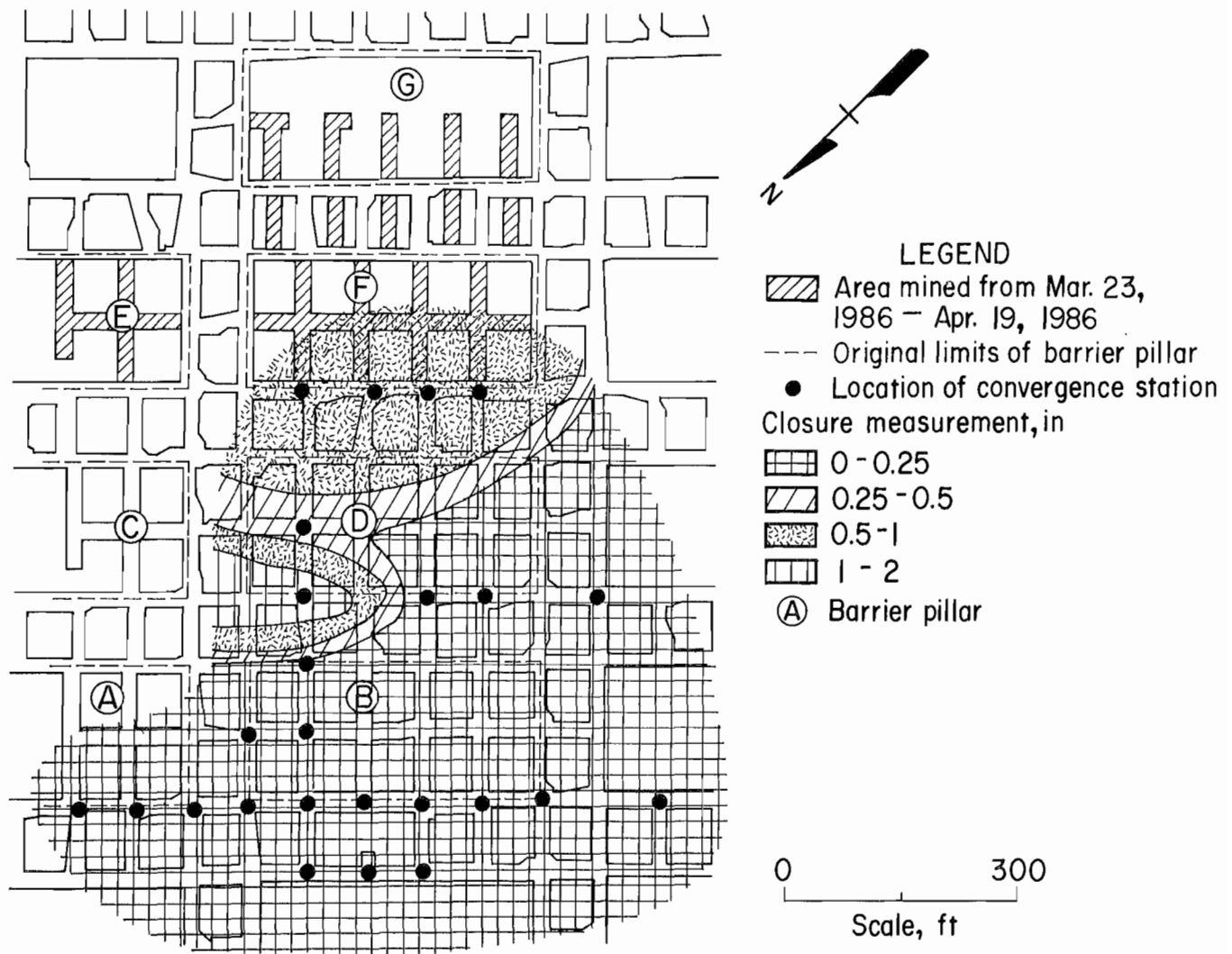


Figure 12.—Isopach map of roof-to-floor convergence from March 23 through April 19, 1986.

splitting began two pillar rows outby the barrier immediately thereafter.

Chain pillar retreat induced a maximum coal cell pressure increase of 5,350 psig and negative pressure changes across the inby most instruments, located in the chain pillars resulting from barrier pillars B and D. The negative changes are presumably due to coal cell failure (fig. 13). These cells failed at an average pressure of greater than 10,000 psi. Maximum roof-to-floor convergence of 13.021 in was measured at the wings adjacent to the gob, in the area of barrier F, with a gradual reduction to no roof-to-floor convergence at the outby solid barriers

(fig. 14). Chain pillars, resulting from barrier pillar B, instrumented with extensometers were located within a zone of 0.000- to 0.250-in roof-to-floor convergence (fig. 14). Minor dilation of less than 0.50 in was noted at the rib of both of these pillars during this period (fig. 15).

Abutment zone loading caused large pressure increases and pillar shortening up to six chain pillar rows outby the newly formed gob (figs. 13-14). The 55- by 70-ft chain pillars were beginning to yield under abutment zone loading. This is in contrast to the rigid behavior of the barriers in earlier periods.

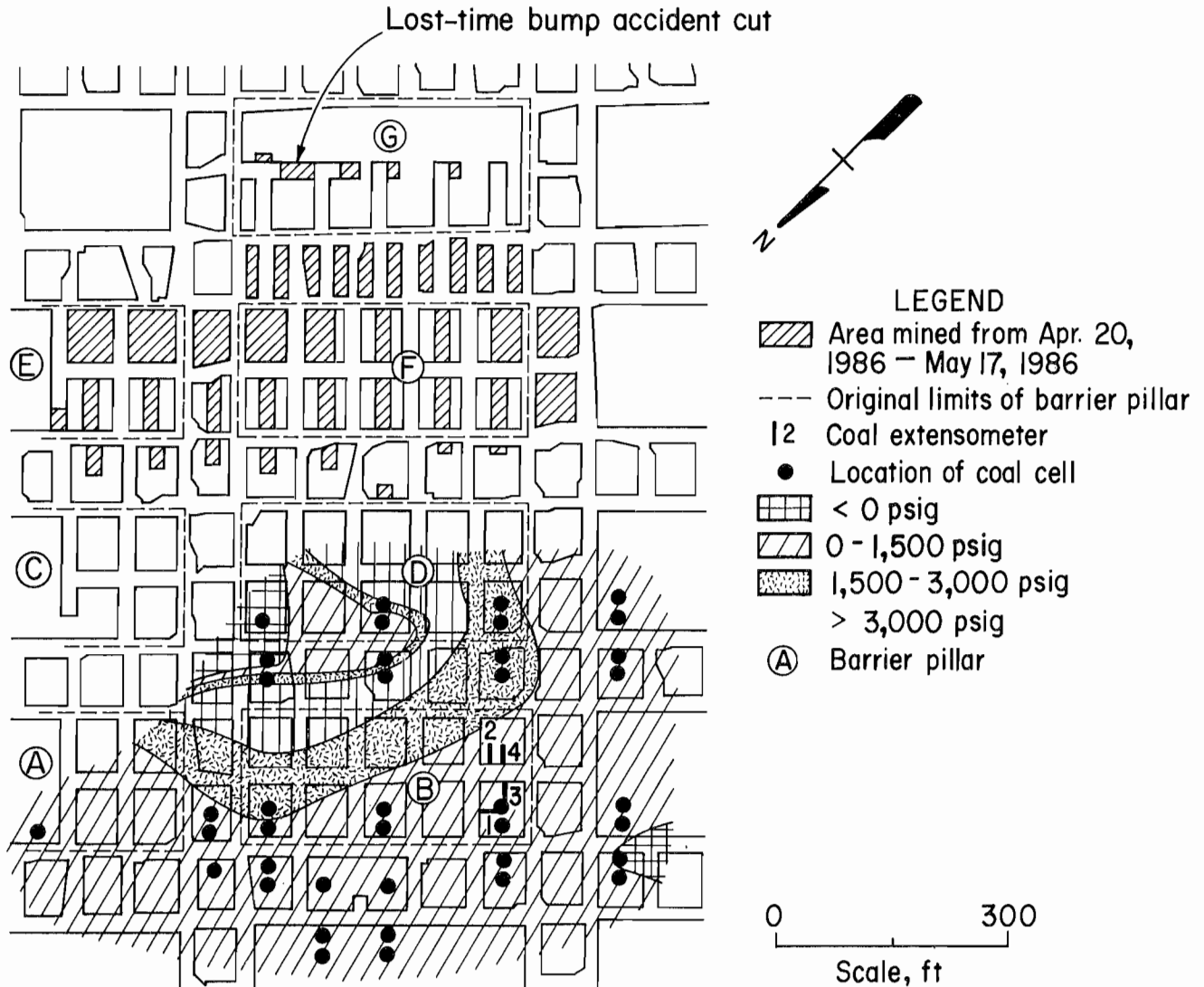


Figure 13.—Isopach map of pressure changes from April 20 through May 17, 1986.

May 18 Through June 14, 1986

The pattern of large increases and negative pressure changes in the inby most surviving coal cells continued during the period from May 18 through June 14 (fig. 16). Many cells exhibiting negative changes were reset with a hydraulic pump, but the pressure continued to fall. However, the areas of coal cell failure and excessive pressure increase (maximum of 4,800 psig) occurred along a diagonal within the section. This pressure pattern developed as

a result of the initiation of a split retreat line. The pillar section was split into two distinct extraction sequences, each made up of four columns of pillars. The left extraction sequence was designed to stay one to two pillar rows ahead of the right extraction sequence. The design change was made in order to decrease the length of the pillar line, thereby limiting the potential for excessive floor heave at the wings adjacent to the gob, as well as shortening the travel distance of the continuous miner between cuts.

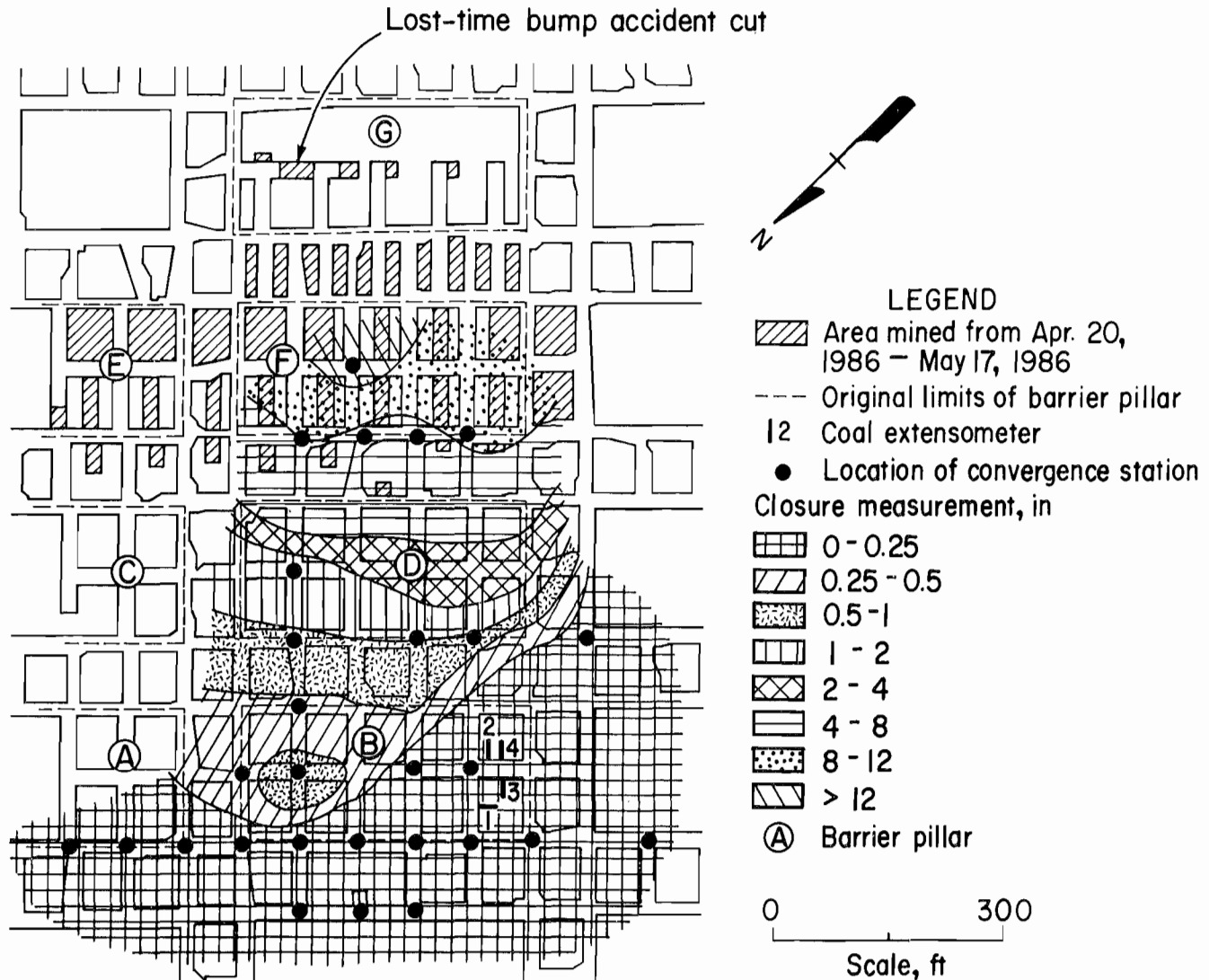


Figure 14.—Isopach map of roof-to-floor convergence from April 20 through May 17, 1986.

Roof-to-floor convergence during this period exhibited a pattern similar to the coal cell response. Both mirrored the stepped extraction sequence. As was the case in the previous period, maximum roof-to-floor convergence (14.234 in) occurred at the wings adjacent to the gob and gradually decreased to less than 0.250 in at the outby solid barrier (fig. 17). Coal pillar extensometer response to the mining was similar to the previous period, with less than 1.00 in of dilation at a 3-ft depth into the pillar, and less than 0.50 in at a 6-ft depth (fig. 18).

June 15 Through July 12, 1986

Mining from June 15 through July 12 induced a maximum coal cell pressure increase of 2,050 psig. Pressure contours were consistent with those of the previous periods and the stepped mining sequence (fig. 19).

The presence of the solid outby barriers condensed the length of the characteristic gradual reduction in roof-to-floor convergence (from a maximum of 9.809 in to less than 0.250 in) to less than 400 ft (fig. 20).

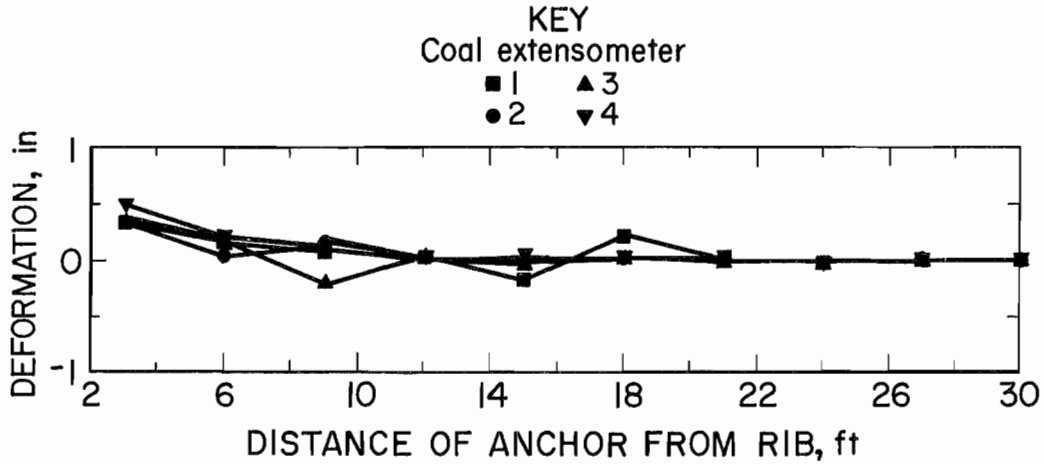


Figure 15.—Dilation of chain pillars instrumented with extensometers from April 20 through May 17, 1986.

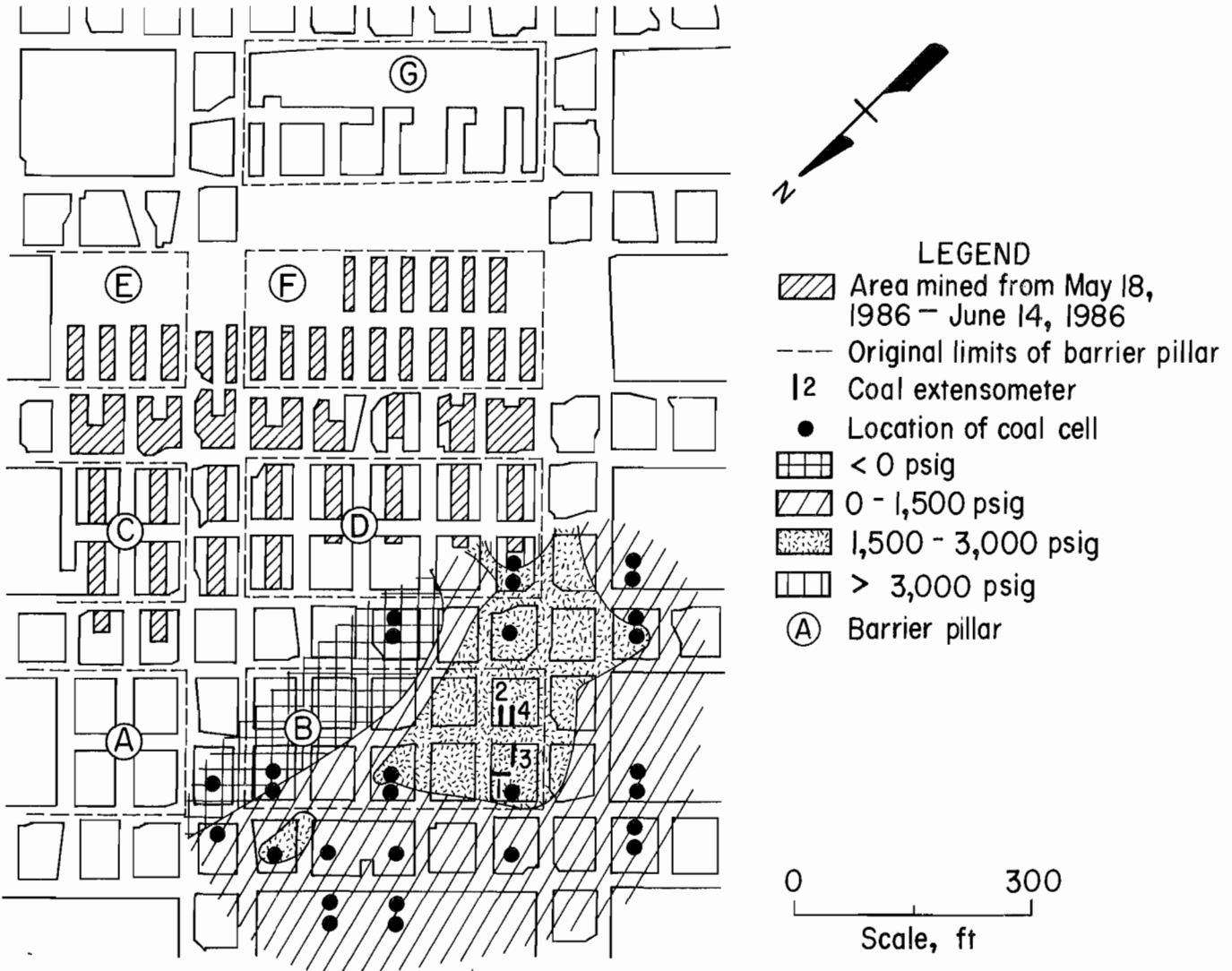


Figure 16.—Isopach map of pressure changes from May 18 through June 14, 1986.

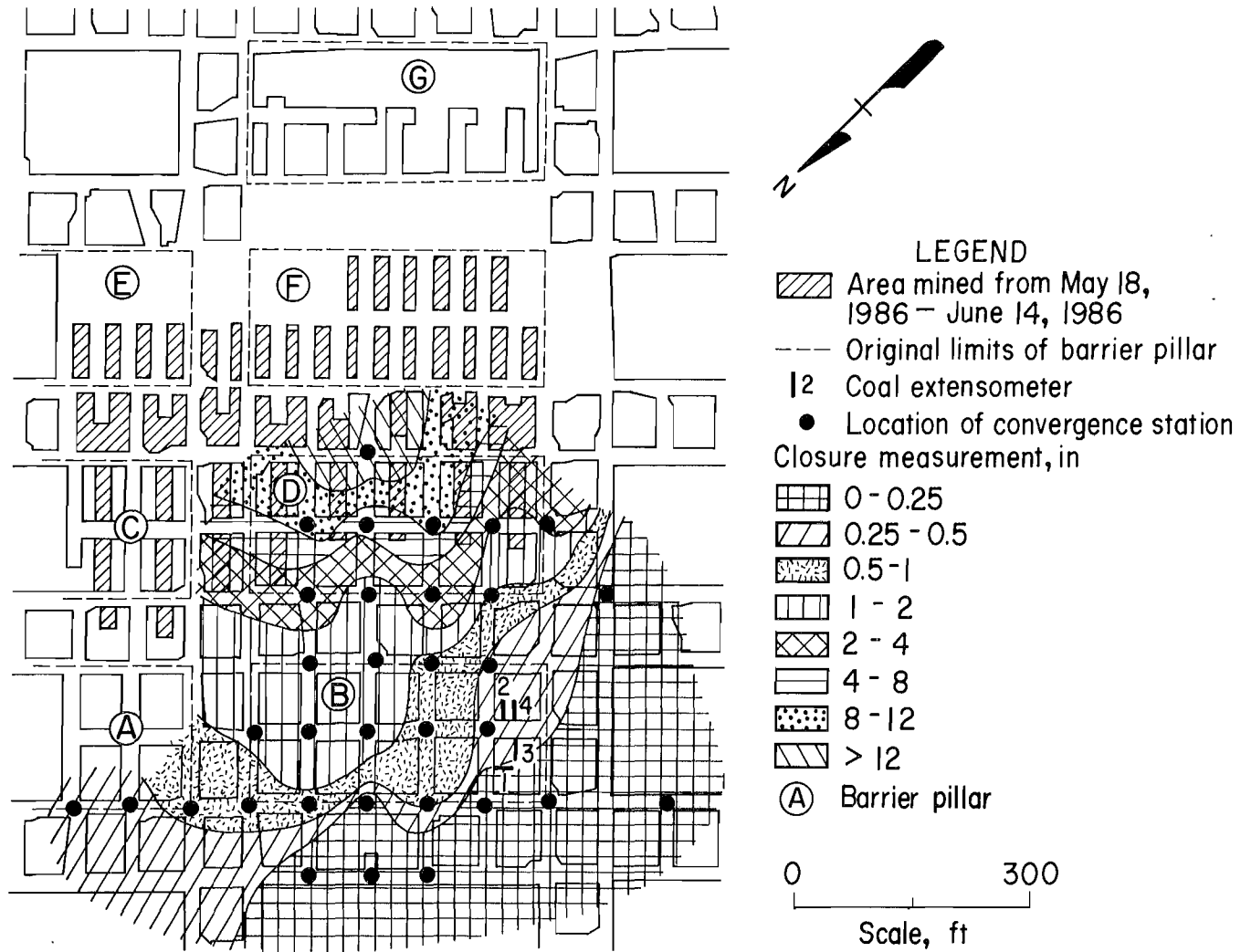


Figure 17.—Isopach map of roof-to-floor convergence from May 18 through June 14, 1986.

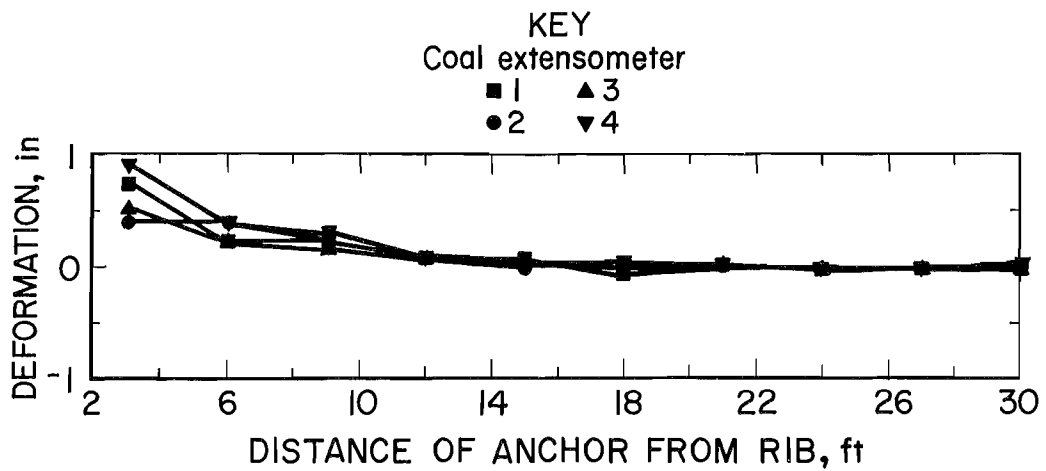


Figure 18.—Dilation of chain pillars instrumented with extensometers from May 18 through June 14, 1986.

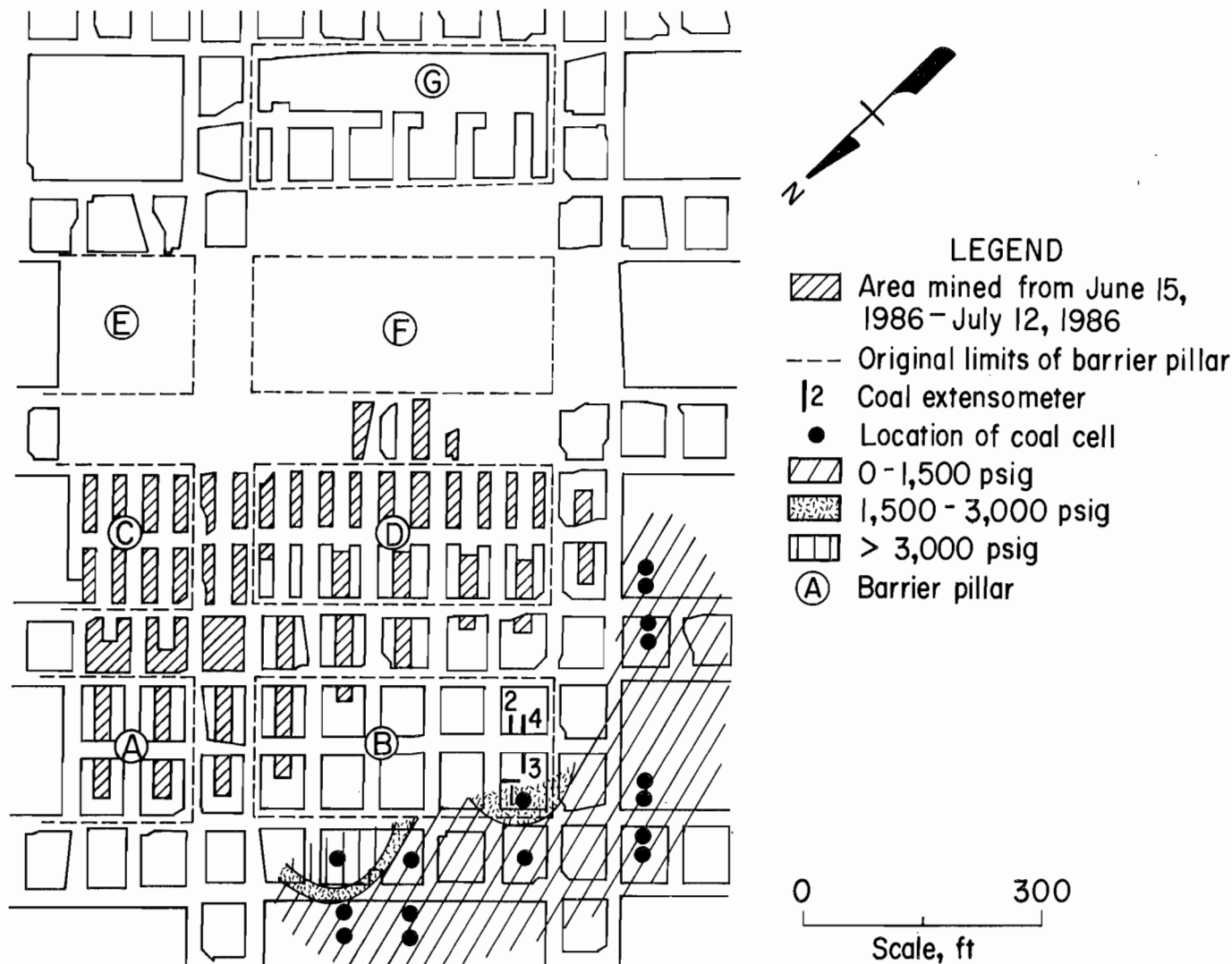


Figure 19.—Isopach map of pressure changes from June 15 through July 12, 1986.

This suggests that the barriers remained stiff and resistant to lateral expansion. In contrast, pillar dilation at a distance of 12 ft into the instrumented pillars occurred for the first time (fig. 21). This was in response to a 1.000- to 0.250-in roof-to-floor convergence in the surrounding entries (fig. 20). The failed 12-ft perimeter confined the pillar core allowing it to sustain pressures greater than 10,000 psig, as measured by the lone surviving coal cell in the extensometer pillars.

July 13 Through August 9, 1986

Because of poor market conditions, no mining occurred from July 13 through August 9. A time-delayed abutment

pressure wave caused a maximum coal cell pressure increase of 1,550 psig in the outby barriers (fig. 22). This is the final period for which coal cell pressure data will be presented. Subsequent data are sparse because of the destruction of coal cells by the progress of mining and the failure of the units at the average threshold of 10,000 to 13,000 psig.

The time-delayed abutment pressure was confirmed by the roof-to-floor convergence data, which gradually fell from a maximum of 2.172 in directly outby the gob to less than 0.250 in at the outby barriers (fig. 23). However, the increased stress levels were insufficient to cause further dilation in the extensometer pillars (fig. 24).

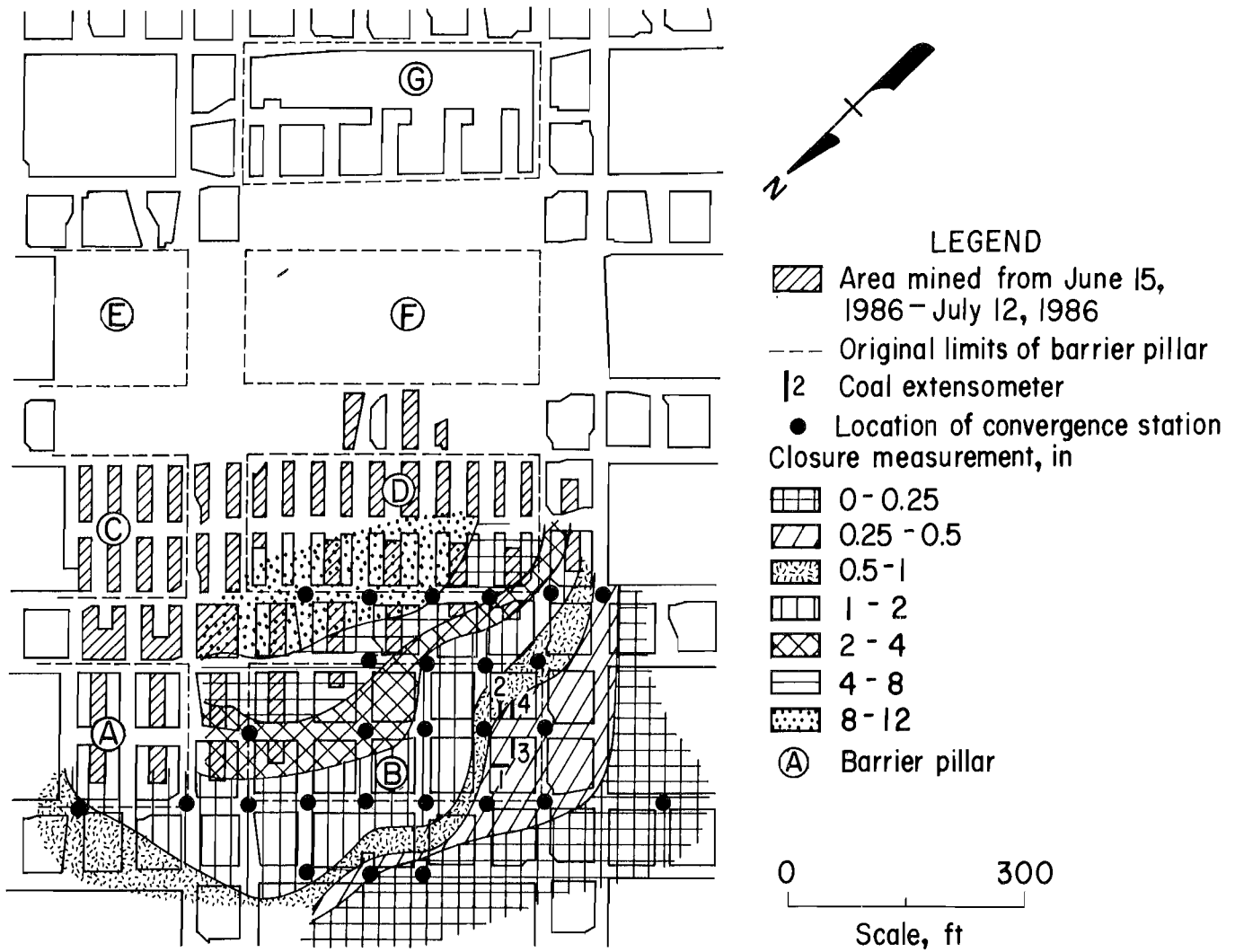


Figure 20.—Isopach map of roof-to-floor convergence from June 15 through July 12, 1986.

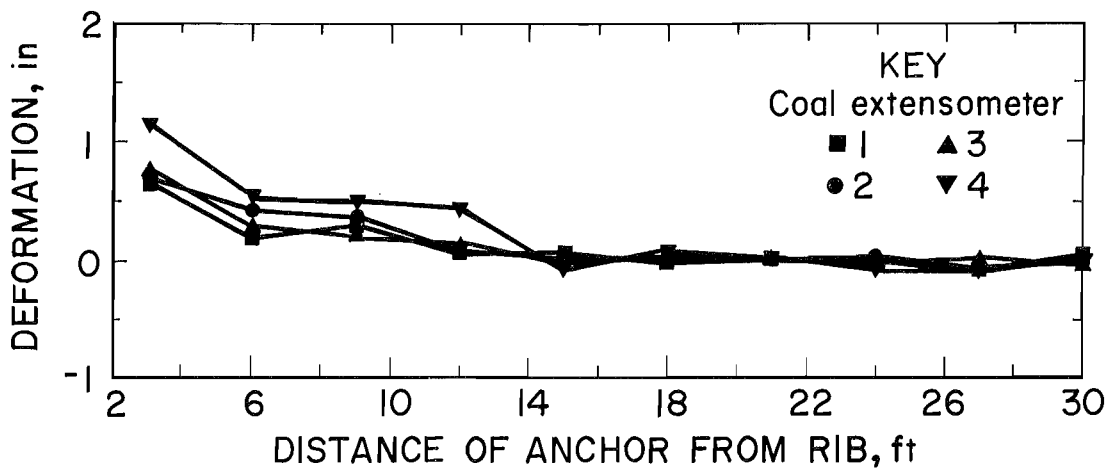


Figure 21.—Dilation of chain pillars instrumented with extensometers from June 15 through July 12, 1986.

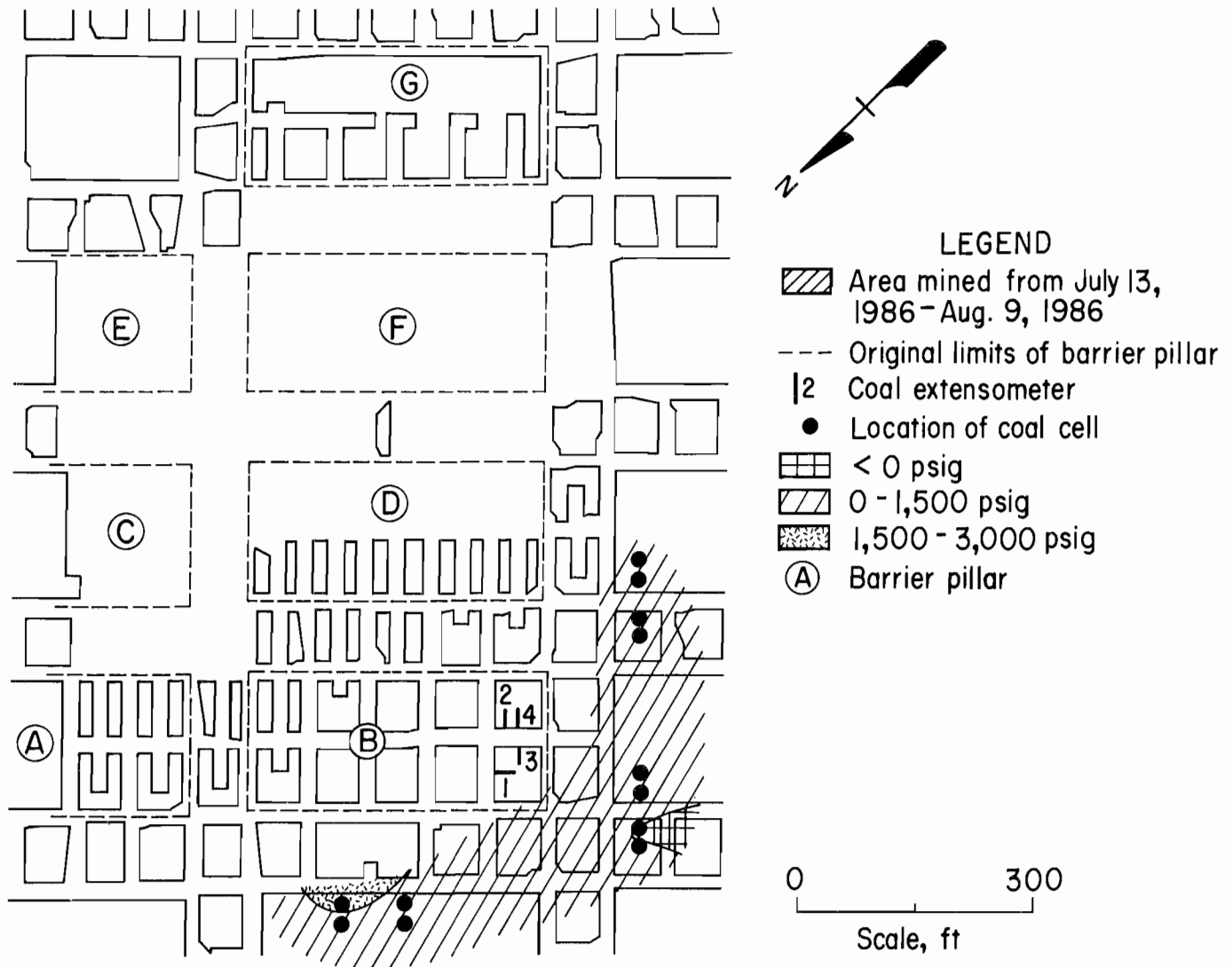


Figure 22.—Isopach map of pressure changes from July 13 through August 9, 1986.

August 10 Through September 6, 1986

A maximum roof-to-floor convergence of 12.399 in was induced by the mining from August 10 through September 6 (fig. 25). The characteristic distance of reduction in roof-to-floor convergence was shortened to less than 200 ft because of the close proximity of the rigid outby barriers. The roof-to-floor convergence contours again were consistent with the stepped mining sequence.

During this period, mining encompassed the chain pillars instrumented with extensometers for dilation measurement. Extensometer 2 was located in a 17.5- by 70-ft wing,

and extensometer 1 was located perpendicular to mining in a partially split pillar (fig. 25). Roof-to-floor convergence in the entries around the two pillars varied from 7.467 to 0.546 in. Mining-induced pillar dilation of over 2.00 in occurred at the 3-ft depth into the instrumented pillars. Less significant movement took place up to 15 ft into both pillars (fig. 26). The anomalous reaction of the 18- and 21-ft anchors of extensometer 1 and the slipping of the 30-ft reference anchors in both extensometers was probably due to the mining of the instrumented pillar. The 15-ft failed perimeter confined the core, permitting the friable coalbed to support extreme pressure.

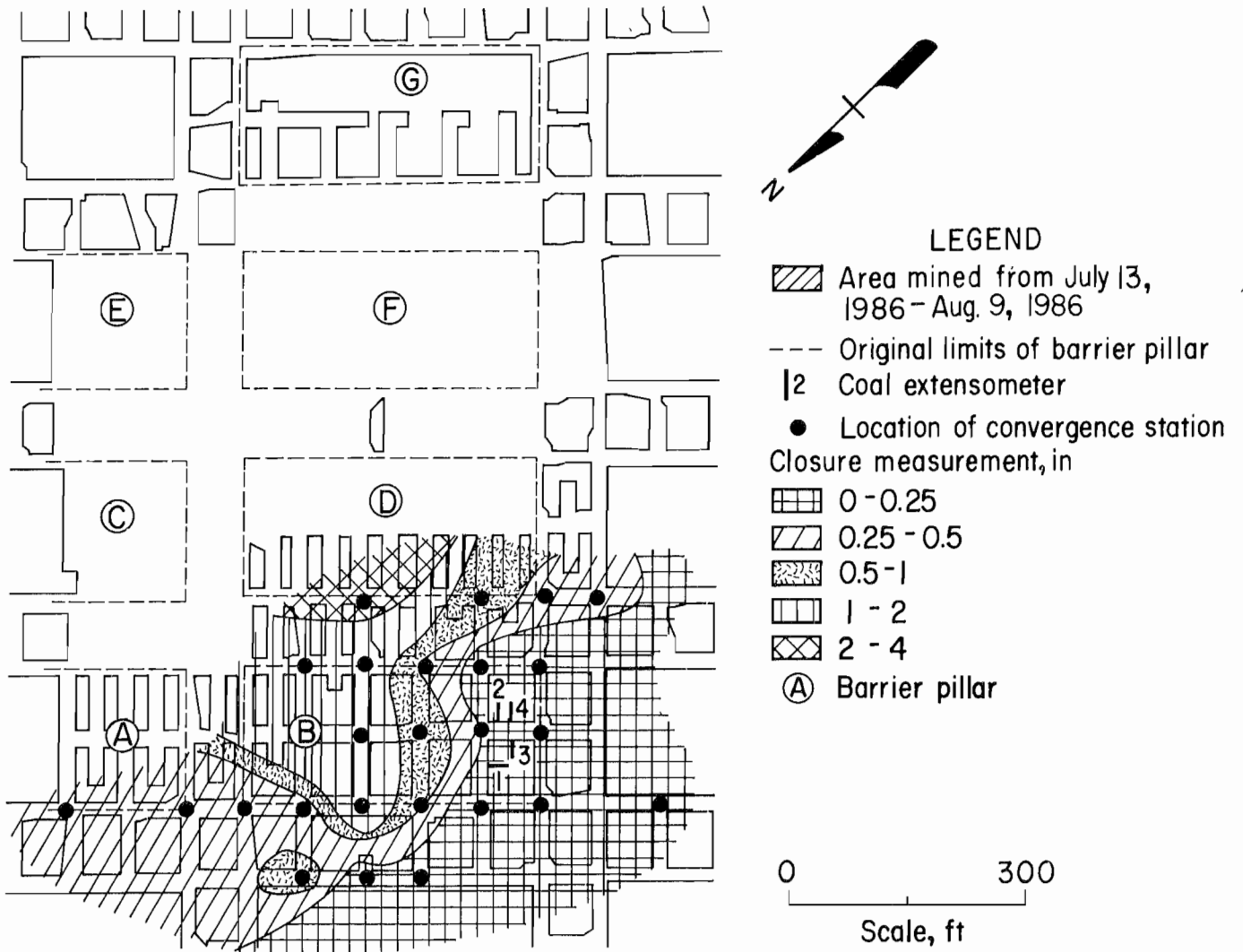


Figure 23.—Isopach map of roof-to-floor convergence from July 13 through August 9, 1986.

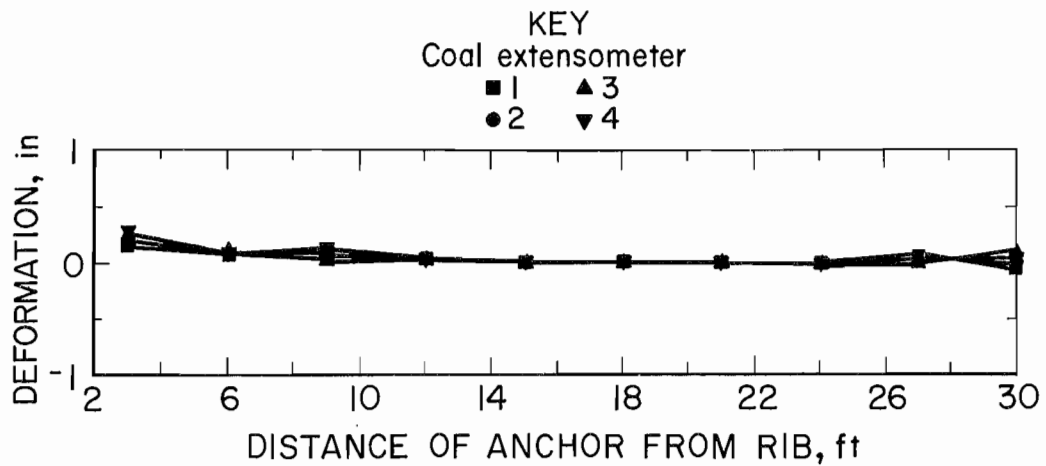


Figure 24.—Dilation of chain pillars instrumented with extensometers from July 13 through August 9, 1986.

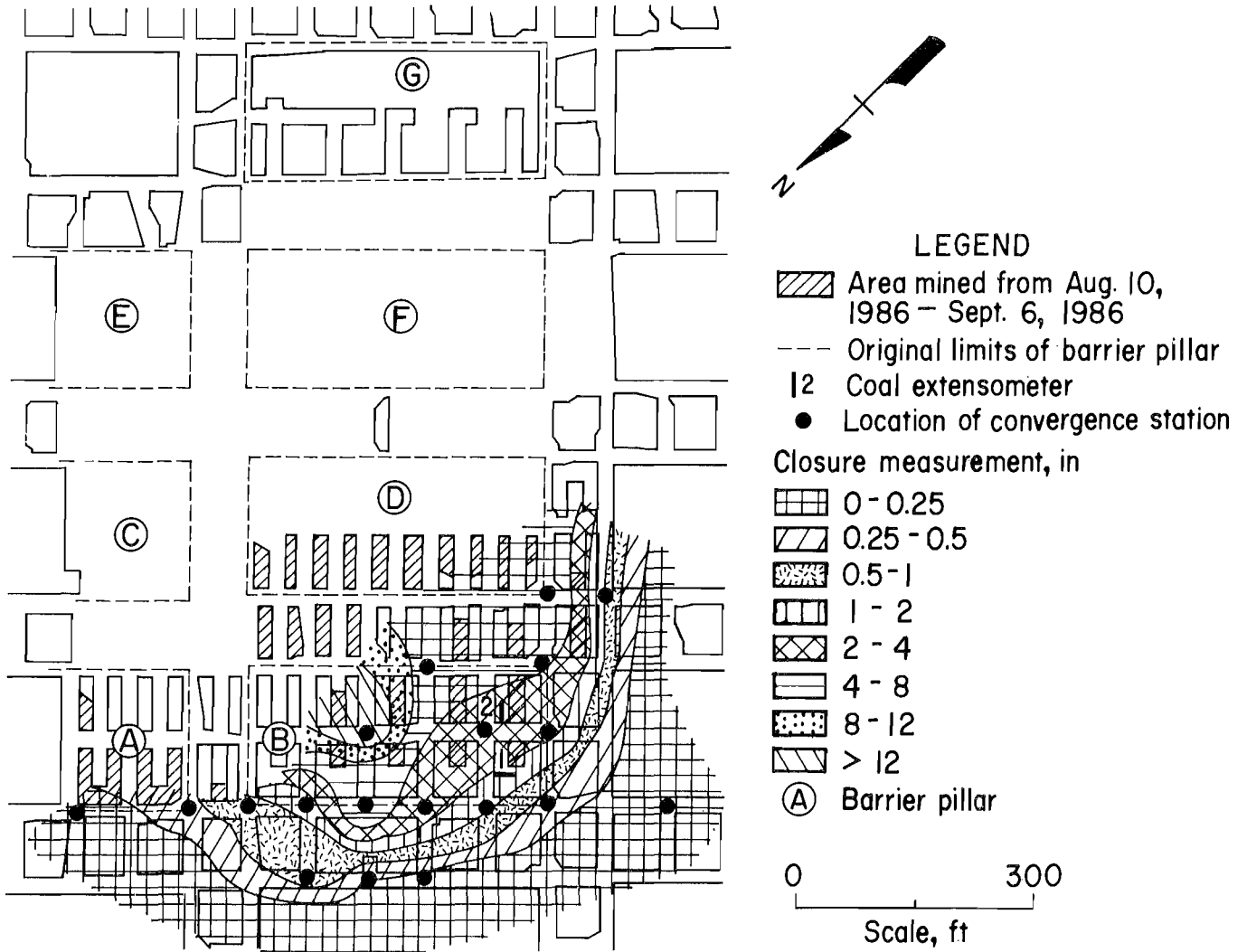


Figure 25.—Isopach map of roof-to-floor convergence from August 10 through September 6, 1986.

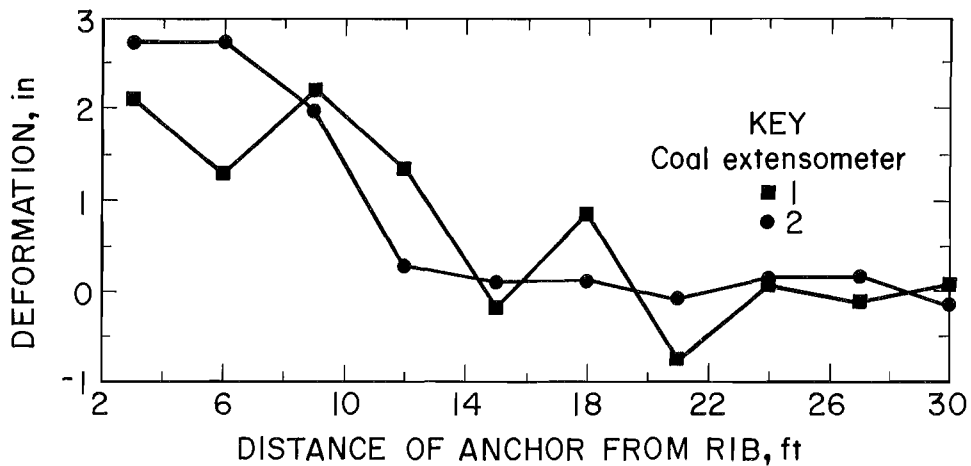


Figure 26.—Dilation of chain pillars instrumented with extensometers from August 10 through September 6, 1986.

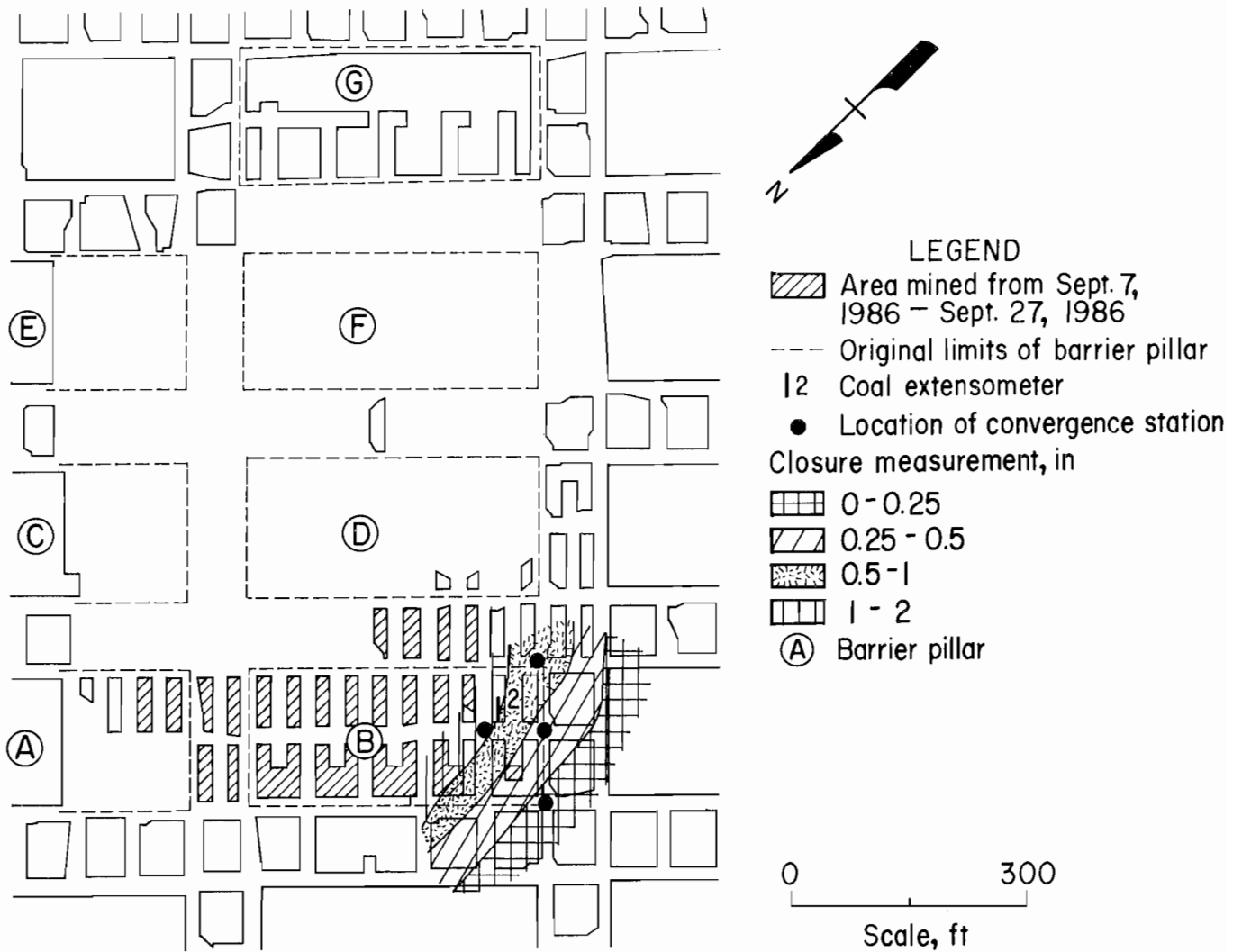


Figure 27.—Isopach map of roof-to-floor convergence from September 7 through September 27, 1986.

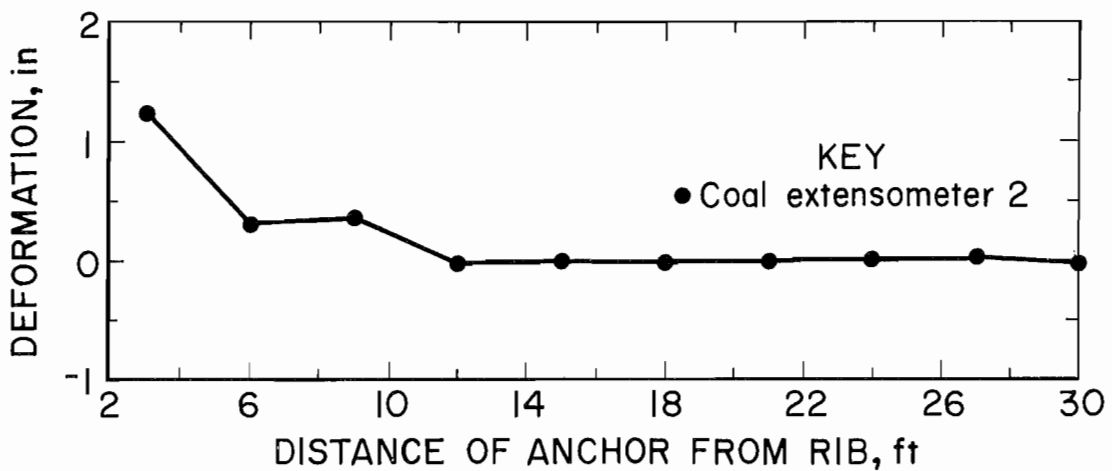


Figure 28.—Dilation of chain pillars instrumented with extensometers from September 7 through September 27, 1986.

September 7 Through September 27, 1986

The final period of mining in the main study area occurred from September 7 through September 27. Because of the very close proximity of the outby barriers, a maximum roof-to-floor convergence of only 1.177 in was induced by mining (fig. 27). The outby barriers were carrying the weight of the nearby gob because of cantilever loading. This illustrates the bump hazard associated with the splitting of barriers under abutment zone loads.

The lone surviving extensometer indicated only 1.25 in of dilation over the first 3 ft of the long axis of the 17.5-by-70-ft wing (fig. 28). It is assumed that dilation occurred around the perimeter of the wing.

HISTORY OF A TYPICAL COAL PILLAR

Detailed analysis of a typical coal cell and the four roof-to-floor convergence stations surrounding an instrumented pillar, provides insight into the relationship between roof-to-floor convergence and coal cell pressure (15). The representative coal cell was located 30 ft into the center of the first barrier pillar to be split. The coal cell was installed 5 months prior to the initial advance mining of the section (fig. 7). Only slight increases in the pillar pressure [to 3,000 psig from the 2,500-psig borehole pressure flatjack (BPF) setting pressure] occurred prior to advance mining of the main study area (fig. 29). Dramatic increases in pillar pressure (to 7,500 psig) and roof-to-floor convergence (2.00 in) were associated with the splitting of the instrumented barrier into ten 55- by 70-ft chain pillars. Coal cell pressure and roof-to-floor convergence readings leveled off during the splitting of the inby barrier pillars. Gradual increases in both coal cell pressure and roof-to-floor convergence occurred when retreat mining began, even though mining was nine chain pillar rows inby.

The maximum measured coal cell pressure of 12,000 psig occurred when mining was five pillar rows outby as shown in figure 7. Immediately thereafter, the roof-to-floor convergence continued around the instrumented pillar but the coal cell began to fail. Final coal cell failure occurred in mid-September after having remained stable during an idle mining period. Many of the cells were reset with a hydraulic pump when they began to lose pressure. None of the cells held the reset pressure, indicating that their bladders were leaking.

DETAILED CONVERGENCE SURVEYS DURING MINING

Immediate roof-to-floor convergence directly outby mining was measured for 61 continuous miner cuts (fig. 30). Entry height to the nearest 0.001 in was measured prior and subsequent to the mining of each 5-st shuttle car load of coal. An average of 15 shuttle car loads were removed from each cut. A characteristic roof-to-floor convergence was associated with each type of cut, indicating the structural capacity of the pillar was changing as mining progressed (fig. 31).

Barrier pillar splitting induced less than an average of 0.003 in of roof-to-floor convergence per 5 st mined. This suggests that the barrier pillars and their resulting chain pillars were resistant to yielding and thus accumulated strain energy. This has been verified by the coal cell data. Splitting the chain pillars into the 17.5-ft-wide wings resulted in the destruction of the load-bearing capacity of the pillar. The load was shed to outby pillars during the first three pillar split cuts, as indicated by the high convergence responses to the bump, second, and third cuts (fig. 31). The pillar carried little load after the third pillar split cut, as demonstrated by the average of less than 0.004 in of roof-to-floor convergence per 5 st mined (fig. 31).

Roof-to-floor convergence was greatest during mining of the wings, averaging over 0.015 in per 5 st mined. This result appears to contradict the earlier statement on the timing of chain pillar yield and associated load shielding. However, the roof-to-floor convergence induced per shuttle car load varied significantly by location within the study area. The other five cut types did not exhibit such behavior.

Figure 32 displays the average roof-to-floor convergence per 5 st mined, for each wing cut survey. The location of the pillar row and column grid is shown on figure 30. The roof-to-floor convergence induced in the middle of the section, pillar columns 4, 5, and 6, is 7.3 times greater than that induced in the remainder of the study area. The 0.0025-in convergence per 5 st mined reading in row H, column 4, is low because of an unmined pillar located directly inby the wing mined. Based on this information, it is theorized that the high roof-to-floor convergence measured in the middle of the section is primarily due to an overall closure of the section at the midpoint of the 600-ft-wide roof span. Thus, the removal of the highly fractured yielded wings does not cause significant stress redistribution.

Five barrier split cuts were surveyed in the 15 working days prior to the bump and the resultant end of advance mining (fig. 33). The surveyed cuts on days 1 and 11 induced an average of less than 0.002 in of roof-to-floor convergence per 5 st mined. This indicated that hazardous strain energy was not present in or around the area of the cuts. The surveyed cut taken on day 14 produced an average of greater than 0.007 in of convergence per 5 st mined. This indicated the presence of strain energy storage in the left side of the inby barrier. The combination of this information and the knowledge that the bump barrier pillar (G) was located at the intersections of two gob areas (fig. 30), led mine management to auger drill what was to be the bump injury cut. The auger drilling was judged to be effective. However, it was insufficient to prevent the bump, which caused an instantaneous roof-to-floor convergence of 1.001 in and an average per shuttle car roof-to-floor convergence of 0.011 in (fig. 33). This further illustrates the extreme bump hazard associated with the splitting of barrier pillars adjacent to gob areas.

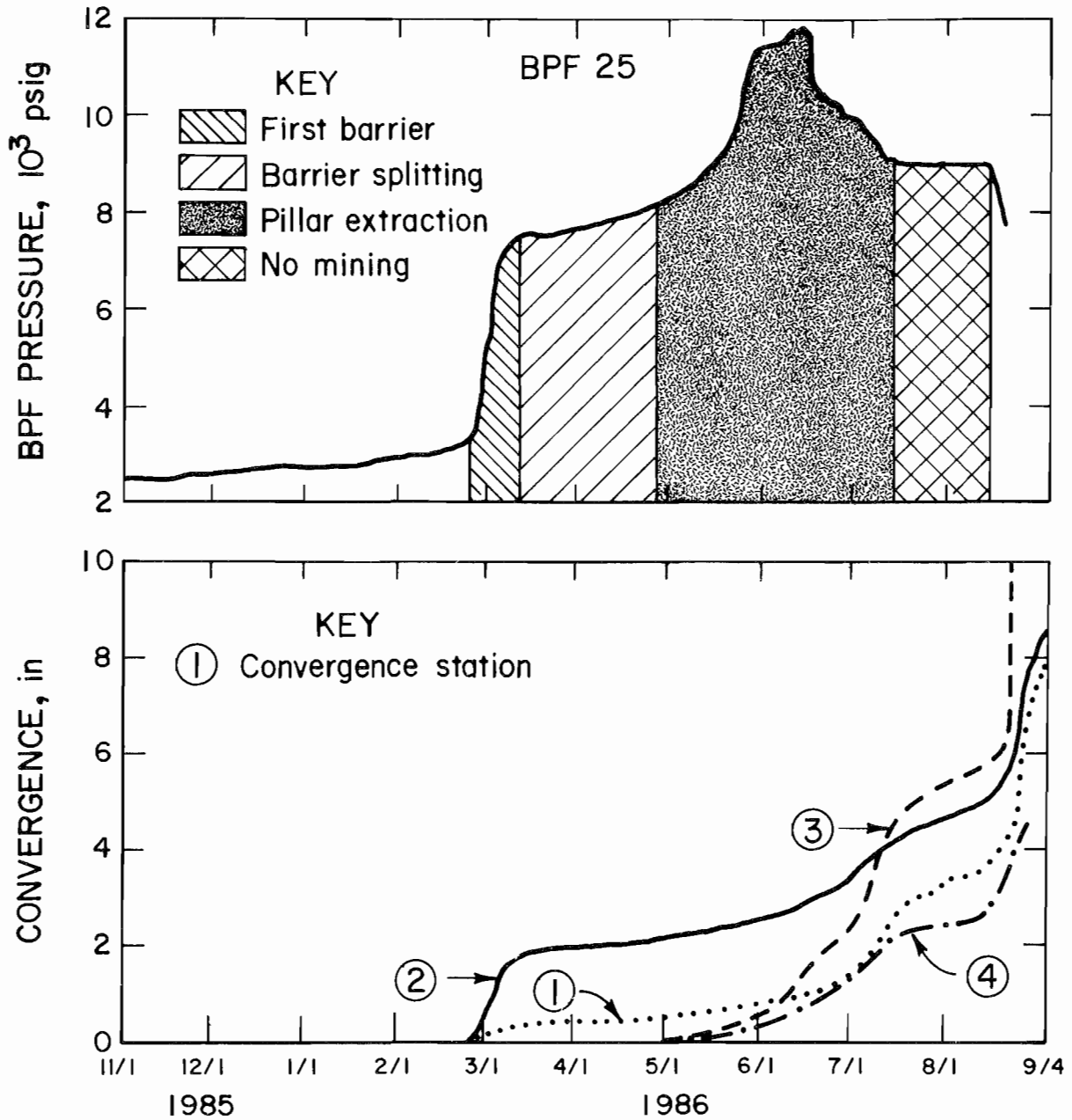


Figure 29.—Coal cell pressure in and roof-to-floor convergence around a typical instrumented chain pillar, from November 1, 1985 to September 4, 1986.

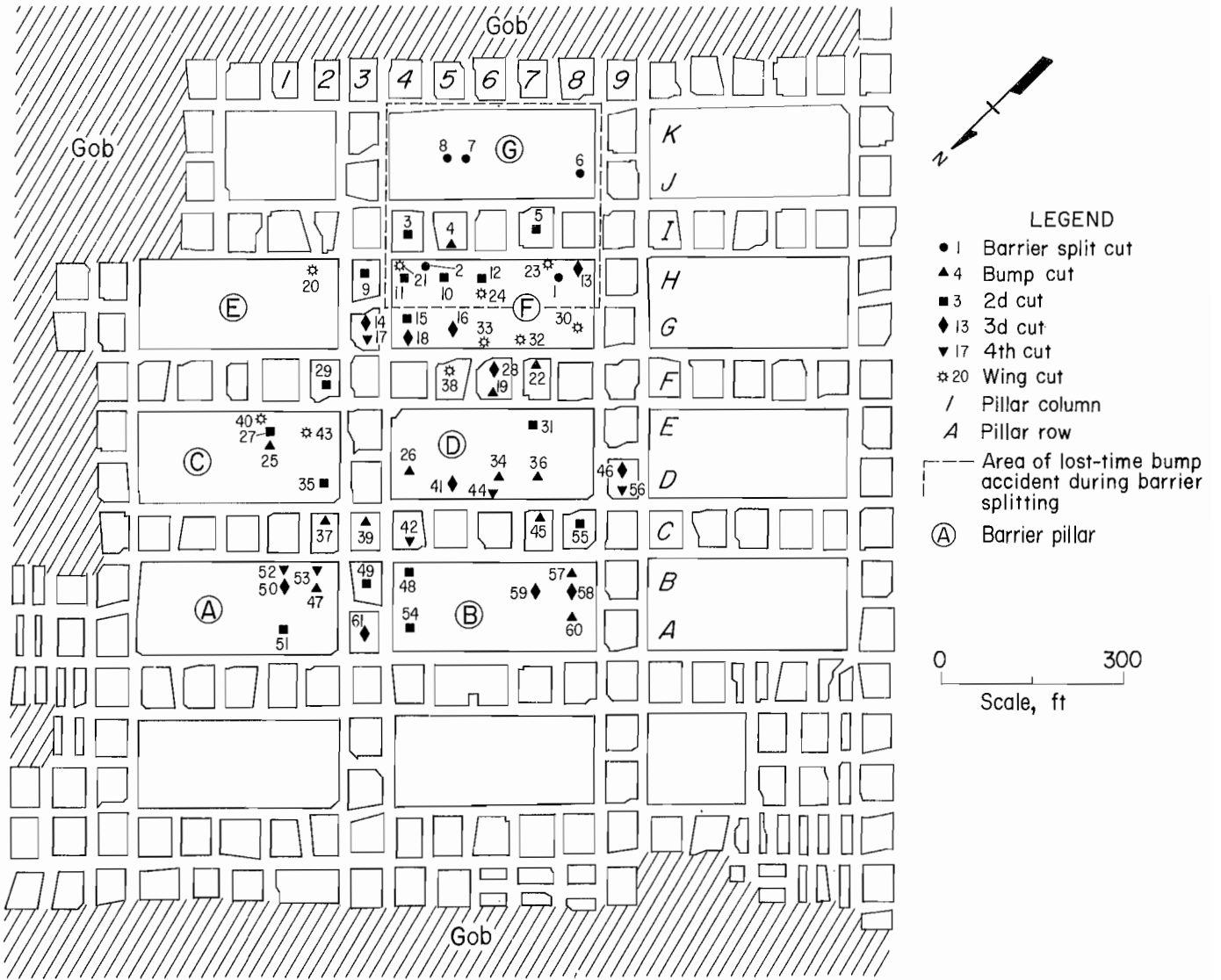


Figure 30.—Map of detailed roof-to-floor convergence surveys.

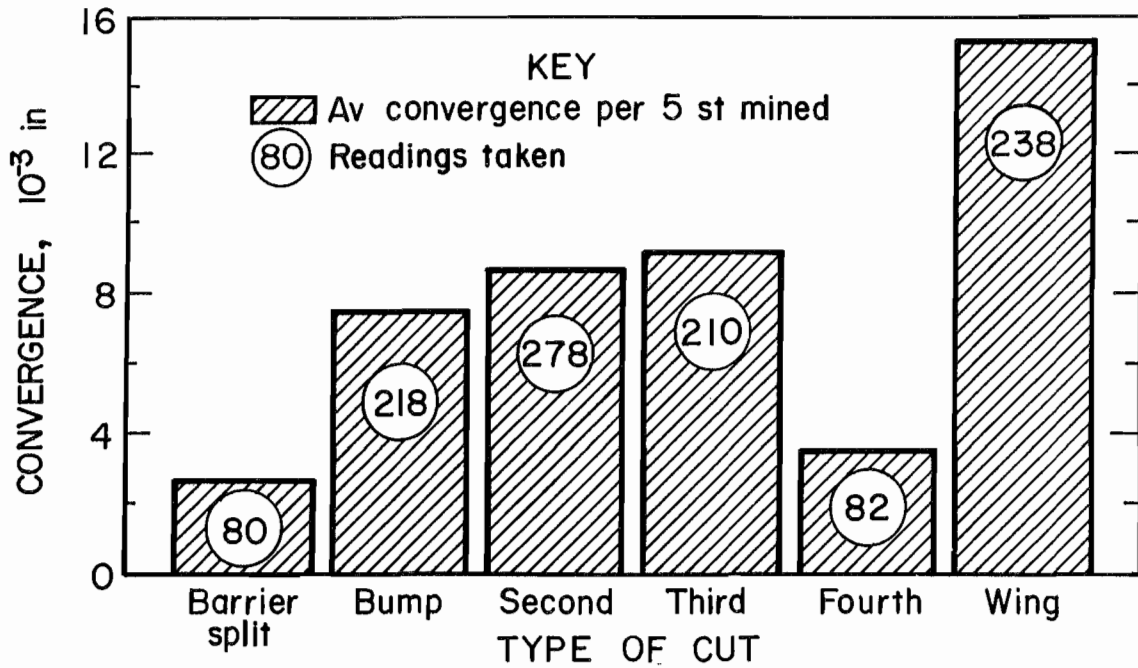


Figure 31.—Detailed roof-to-floor convergence versus cut type.

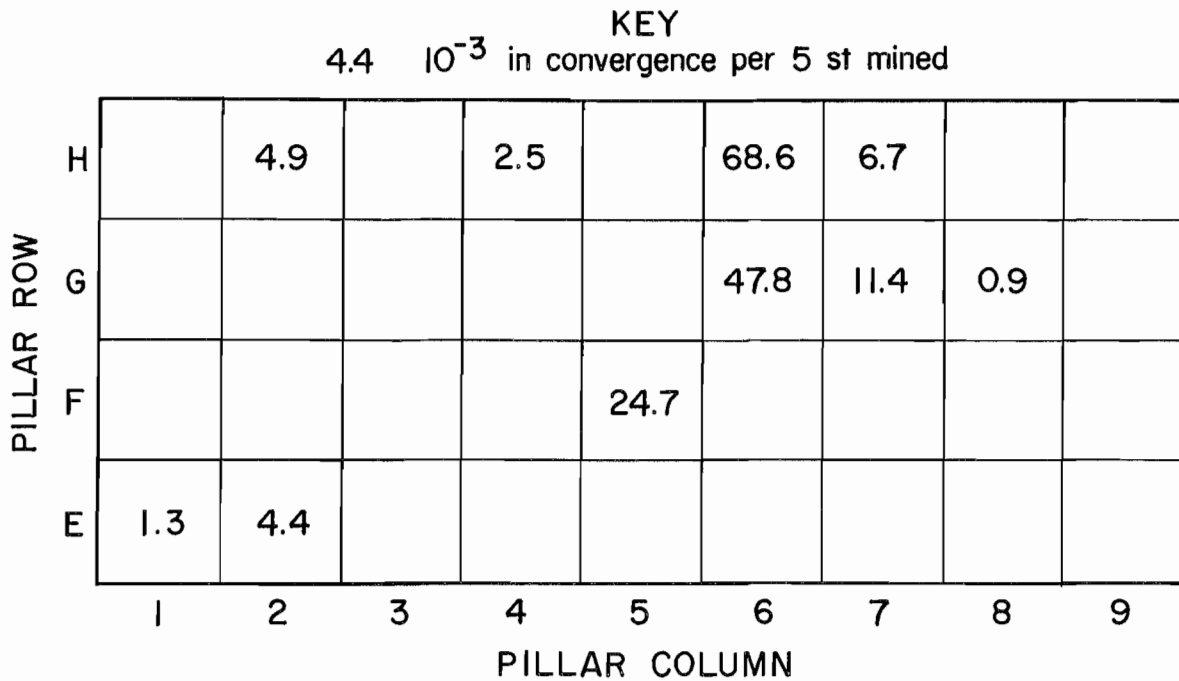


Figure 32.—Illustration of location sensitivity of wing cut detailed roof-to-floor convergence surveys (see figure 30).

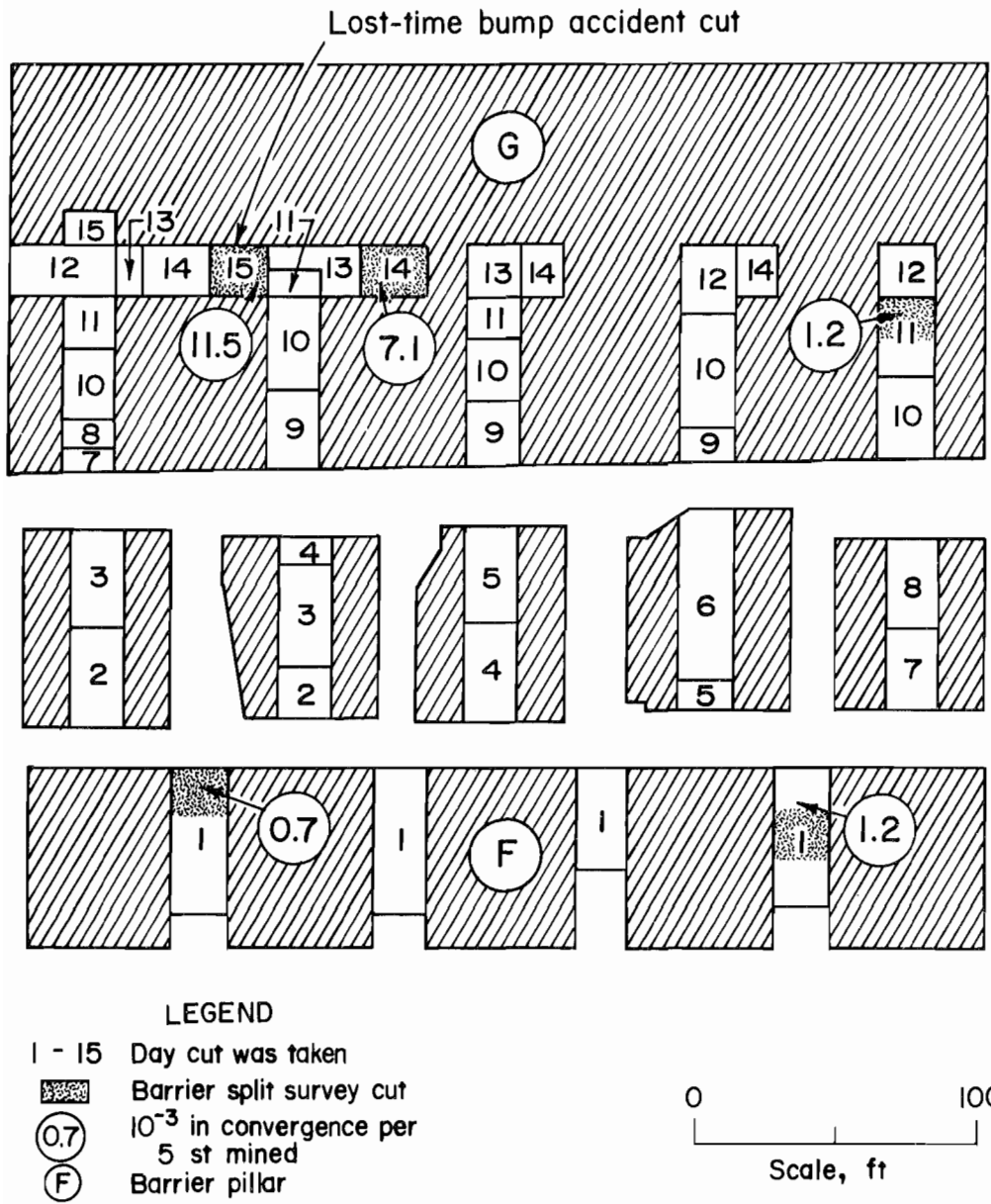


Figure 33.—Barrier split cut detailed roof-to-floor convergence surveys in area of lost-time, barrier-splitting bump accident.

REACTION OF ASSOCIATED STRATA TO MINING

The reaction of the roof and floor strata to mining was evaluated through the use of extensometers to measure roof separation and floor heave. The Bureau's borehole deformation gauge was used in vertical roof core holes to measure the horizontal components of in situ stress. These measurements were made before retreat mining began, so they did not give any indication of the effects of retreat mining. A Commonwealth Scientific Industrial Research Organization (CSIRO) hollow inclusion cell was also installed in one of the core holes to allow measurement of changes in the stresses in the roof rock during mining.

IN SITU HORIZONTAL ROOF STRESS

The Bureau's borehole deformation gauge was used in vertical core holes drilled into the roof to measure the horizontal components of in situ roof stress. Two holes were drilled in the 9 Right section and another in the 8 Right section, which is located 2 miles from the 9 Right section (fig. 3). The average horizontal principal stresses were determined to be 3,000 psi at N 60° E and 2,000 psi at N 30° W. A more complete discussion of borehole deformation gauge procedures and results is contained in the appendix.

The stresses measured at the Olga Mine were compared to stresses determined between 1978 and 1980 by Tosco Research, Inc., under a contract with the Bureau of Mines (16). The measurements taken during the Tosco study were also obtained by overcoring the borehole deformation gauge in vertical holes drilled into the roof. The mines in the Tosco study were north of and within 70 miles of the Olga Mine. However, the overburden depths were 830 to 1,150 ft as compared to over 1,600 ft at 9 Right and 1,250 ft at the 8 Right section. Also, the Tosco measurements were taken in rock above the Beckley Coalbed.

As reported by Tosco, the average maximum horizontal stress measured was 3,260 psi at N 64° E. The average minimum principal horizontal stress was 2,500 psi. These stresses are similar to the average measured at the Olga Mine, both in magnitude and direction. This close agreement in different locations suggests that the stresses measured at all of these sites were produced by regional tectonics. It also suggests that the measurements were only slightly affected by differences in mining activity, rock type, and overburden depth. Thus, horizontal stress was deemed not to be a contributing factor in causing bumps at the Olga Mine (15).

RELATIVE MINING-INDUCED PRESSURE CHANGES IN THE ROOF

A CSIRO hollow inclusion cell (17) was installed on February 28, 1986, in roof hole 6 at a depth of 13 ft (fig. 6) and changes in strain were read periodically through October 2, 1986. The results represent the direction and magnitude changes in the three-dimensional stress field, from the date of installation. The results were obtained without overcoring.

Data from numerous hollow inclusion cells overcored at the Olga Mine were compared with the Bureau's deformation gauge results, also obtained at the Olga Mine. The hollow inclusion cells gave similar stress directions but much lower stresses. The following discussion is presented under the assumption that the hollow inclusion cell is effective only in determining mining-induced changes in the direction of the principal stresses in the host rock, and relative changes in the magnitude of the stresses.

Between February 28, when the permanent cell was installed, and May 14 all three principal stresses showed rapid increases (fig. 34). Since the greatest increases took place before April 22 when barrier splitting was terminated, it appears that most of the stress increase was in response to the barrier splitting operations.

By May 14 the vertical principal stress had increased by 900 psi, and the horizontal principal stresses had increased by 1,700 and 1,500 psi. After May 14, the stress seen by the cell showed only minor changes through June 25. On June 26 and 27, the 55- by 70-ft pillar immediately adjacent to the cell was split into two 17.5- by 70-ft wings. The next cell reading on July 2 shows a reduction of the vertical stress change of over 300 psi and a rotation of the horizontal principal stress directions, though only slight changes in their magnitudes. From that time until the last cell reading on October 1, the vertical stress change gradually dropped until the vertical stress seen by the cell was essentially the same as when the cell had been installed. Horizontal principal stress changes of about 1,700 psi continued to be present through October 2, 1986. The formation of a roof cantilever, spanning the midsection gob and the adjacent barrier pillar, appears to permanently affect the direction and magnitude of the horizontal roof stress. The drop in vertical pressure was coincidental with the rotation of the horizontal roof stress direction.

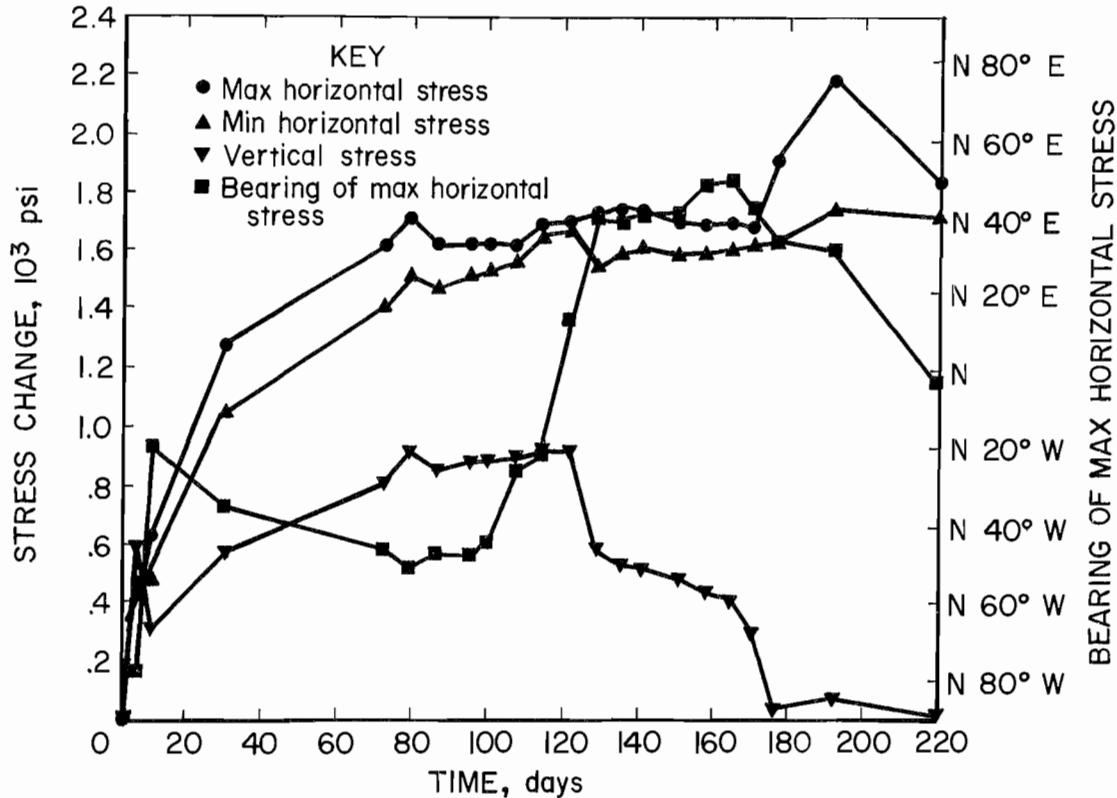


Figure 34.—Hollow inclusion cell principal stress data, from February 25 to October 2, 1986.

MINING-INDUCED ASSOCIATED STRATA MOVEMENT

Measurement of associated strata movement induced by mining was accomplished with two multipoint roof extensometers, boreholes 1 and 7 (fig. 6), and two single-point floor extensometers, boreholes 2 and 8 (fig. 6). The 25-ft-long roof extensometers consisted of five anchors at 5-ft intervals. The floor extensometers measured total movement over the first 20 ft of the floor. No

significant movement was observed in any of the extensometers. Floor movements of only 0.06 and 0.31 in occurred during the entire mining period. The total roof movements at boreholes 1 and 7 were 0.03 and 0.36 in, respectively. Convergence measured in the rooms containing the roof and floor extensometers was a result of bending of the main roof, above 25 ft into the roof. Thus, both the roof and floor acted as large thick plates during the entire mining period.

LOCALIZED DESTRESSING TECHNIQUES

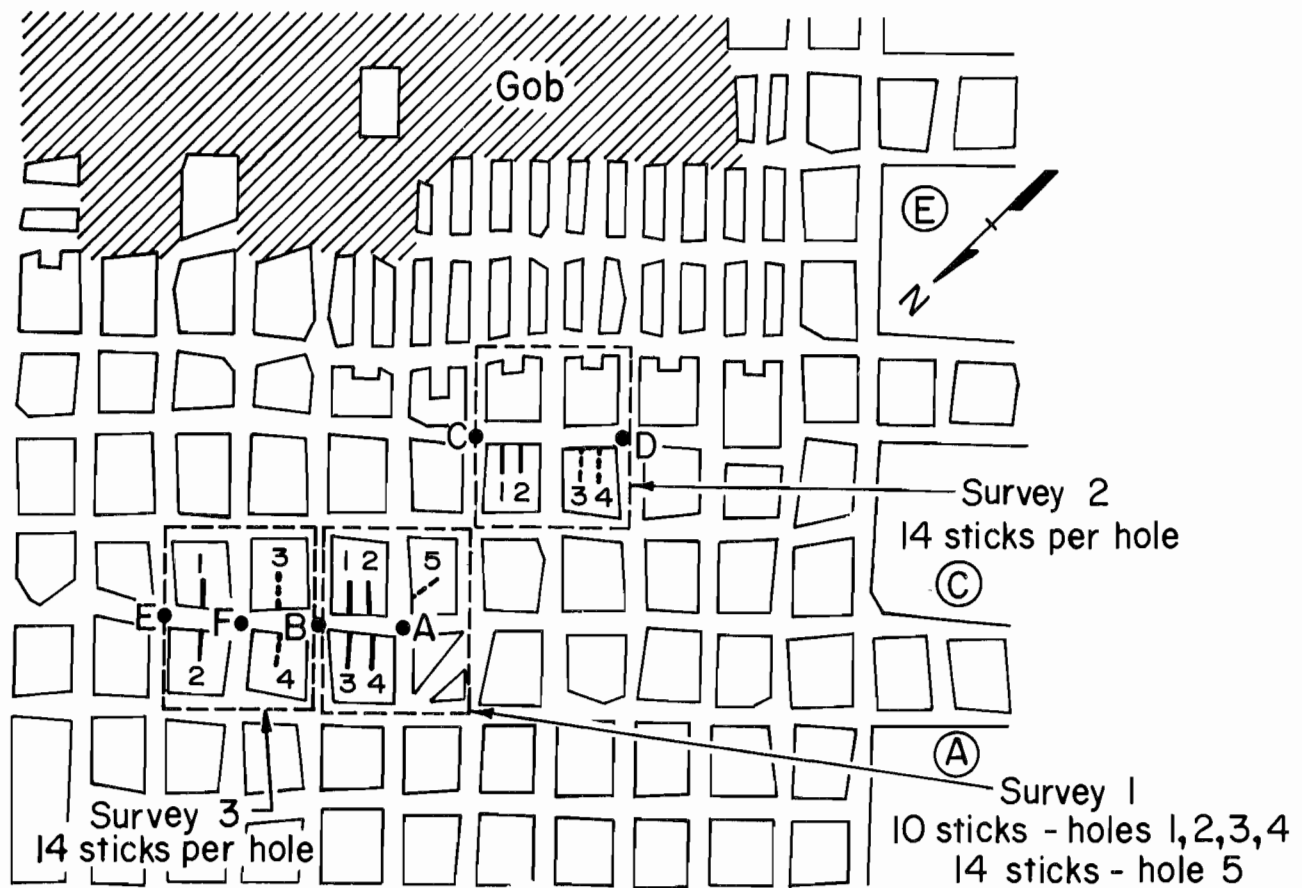
Shot firing, auger drilling, and water infusion have been employed for localized destressing in bump hazard pillars (18). A limited number of auger drilling and shot firing operations were conducted in the study area (19). Critical to destressing success is the location and timing of pillar

treatment. Detailed convergence survey data were used by the mine operators to pinpoint the most effective location and timing for localized stress relief auger drilling. The second and third chain pillar split cuts just prior to mining were targeted for the auger drilling.

SHOT FIRING

Shot firing was employed at the Olga Mine to reduce the load-bearing capacity of coal pillars; and thus, their potential for strain energy storage (19). Three shot fire experiments, conducted in advance of pillar splitting retreat mining, were evaluated by roof-to-floor convergence monitoring on October 11, 1985, in the area to the right

of barriers A and C (figs. 35 and 6). Red Diamond Gelatin B permissible dynamite was used. The blasting agent has the following characteristics: (1) density, 1.35 g/cm³; (2) detonation rate, 16,000 ft/s; (3) detonation pressure, 81,000 bar; (4) weight strength, 955 cal/g; and (5) weight per stick, 211 g. The high detonation rate ensures that a heavy shock wave will fracture the coalbed with minimal movement of the coal.



LEGEND

- A - F Convergence station locations
- 1 - 5 Shot fire holes
- Hole shot in 1st volley
- - - Hole shot in 2d volley
- Ⓐ Barrier pillar

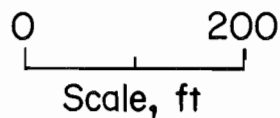


Figure 35.—Shot fire roof-to-floor convergence survey locations and hole configurations.

AUGER DRILLING

Each experiment consisted of two shots. Roof-to-floor convergence station location, hole configuration, and dynamite load varied in the three experiments (fig. 35). The experiments were completed in sequence, within a 6-h nonmining period. Figure 36 graphically displays the convergence induced. Roof-to-floor convergence due to mining was considered negligible. This is confirmed by the stabilization of the roof-to-floor convergence readings between shots.

All three experiments show a roof-to-floor convergence reaction to both shots. This may indicate a softening of the subject pillars because of shot firing, resulting in a reduction of their energy storage. The minimum and maximum roof-to-floor convergence reactions occurred during test 1 in reaction to the minimum (14 sticks) and maximum (40 sticks) dynamite loads. This suggests that the effectiveness of shot firing increases with the amount of explosives used. Other important variables not considered are pillar geometry, hole spacing, and the effect of simultaneous treatment of multiple pillars.

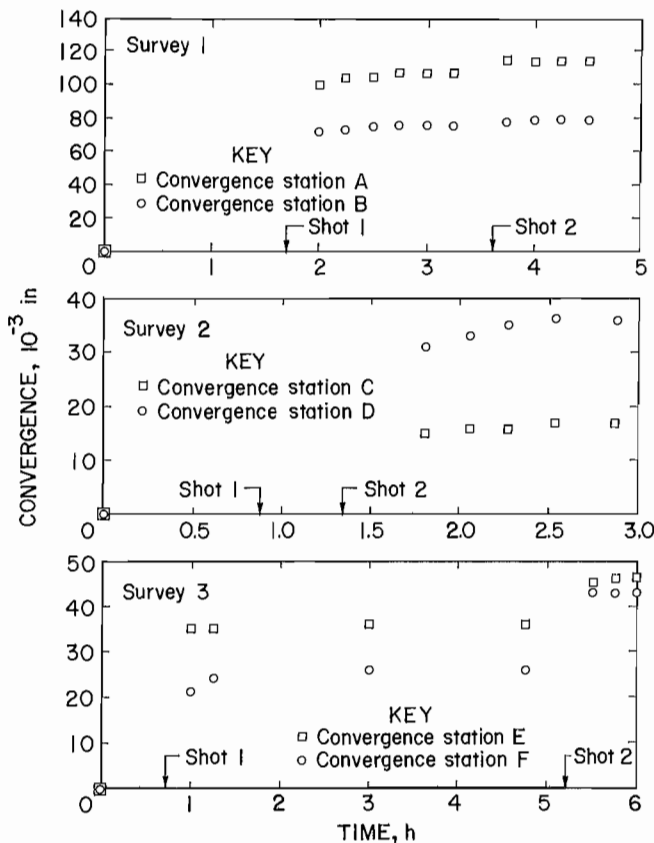


Figure 36.—Roof-to-floor convergence versus time for shot fire surveys 1, 2, and 3.

Dry auger drilling was also used for localized stress reduction at the Olga Mine. The unit employed was a post-mounted, air-driven drill capable of achieving a maximum torque of 447 ft·lbf, consuming 320 ft³/min of compressed air at 58 psi working pressure. Compressed air drills are preferred over electrohydraulic units because air drills provide their highest torque when stalled, providing a high probability of freeing stuck augers. Also, exhaust air helps dilute any methane produced by drilling. Auger drill rod (40 in long) rotated at a maximum of 325 rpm during drilling. A 3.9-in-diam bit was followed by pin-connected augers that had flight and steel diameters of 3.6 and 2.4 in, respectively. All the holes were drilled at mid-seam height. Drilling was remotely controlled 60 ft away from the face. Workers were at the face only to change steel. To further enhance safety, the auger was designed to allow rotation in either direction to minimize human exposure at the coal face in the event the drill string became stuck in the pillar.

Dry cuttings were removed by the right-hand screw action of the augers and air blown through the steels. The volume of cuttings was measured as an indication of stress encountered at the drill depth. At the end of each steel length of penetration (40 in), the cuttings produced were shoveled into a 5-gal bucket. Measurements of this type are commonly used in Europe to evaluate the effects of destressing techniques (20), and to identify hazardous areas in advance of mining (21). A large volume of cuttings is thought to indicate highly stressed coal pillars, hence bump hazard zones.

Eleven auger drilling experiments were monitored for cuttings volume yield and induced convergence effects. The experiments were performed within the period from February to September 1986. Figure 37 gives the 11 test sites on a map of the section prior to mining. The geometry of the section was different for each test, thus figure 37 only locates the test sites geographically. Each experiment was completed in less than 2 h. The holes averaged 24 ft in length.

The tests were conducted under four different mining conditions. Five tests were performed in chain pillars within three chain pillar rows of the gob. Two tests were in chain pillars within six chain pillar rows of the gob. One test was in a chain pillar located between two barrier pillars. Three tests were conducted in advance of barrier splitting cuts. Roof-to-floor convergence caused by sources other than auger drilling was considered negligible. Varying the bit size or drilling multiple holes in a single pillar would affect results, but neither were done during this study.

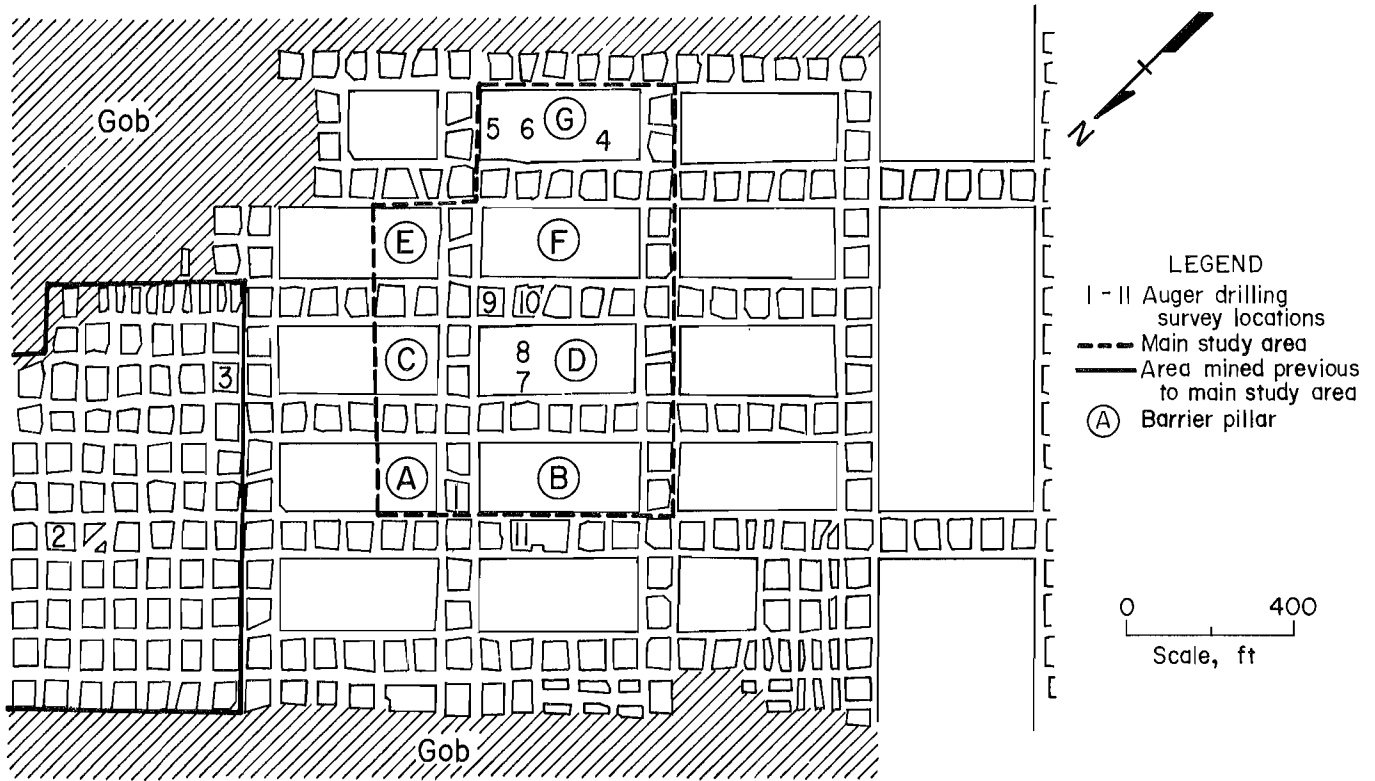


Figure 37.—Auger drilling survey location map.

A graph of the induced roof-to-floor convergence versus the cutting volume produced by each of the 11 auger drill operations reveals that a direct relationship exists between the data sets. The equation $y = 0.06(x) + 9.6$, using the units gallons for the x axis and 0.001 in for the y axis, is plotted with the associated 95-pct-confidence interval for all 11 tests (fig. 38). The wide confidence interval is partially a result of the difference in the pillar stress conditions at the time of the tests. The correlation is also weakened by test 8, which fell well outside of the confidence interval by producing 0.129 in of convergence for 454 gal of cuttings. The equation fit to the data predicts only 0.037 in of convergence for 454 gal of cuttings. If test 8 is ignored, the R-square value for the equation is 0.89.

Test 8 test was conducted during the drilling of a chain pillar located three chain pillar rows outby the gob prior to the first chain pillar split cut. It is unique in that a bump was induced at a drill depth of 28 ft. The bump expelled sufficient coal to block a shuttle car haulway and produced an almost instantaneous roof-to-floor

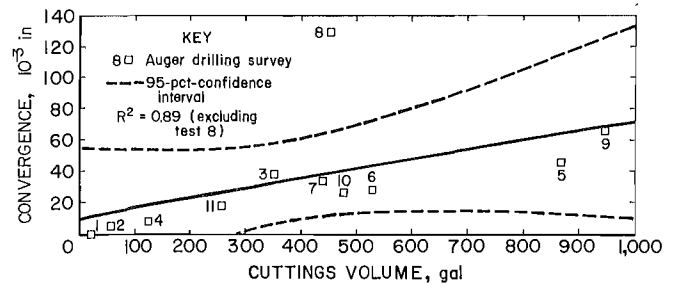


Figure 38.—Total roof-to-floor convergence versus total cuttings volume produced for 11 auger drilling surveys.

convergence of 0.101 in. This is an example of the energy that can be released by auger drilling. Because of safety precautions taken, no injuries were incurred in any of the drilling operations.

The effectiveness of auger drilling for destressing proved to be dependent on the state of stress within the treated pillar. Survey 1 was performed in a 55- by 70-ft chain pillar located between two barrier pillars (fig. 39). The pillar was located within an array of coal cells and roof-to-floor convergence stations. At the time of this experiment, raw readings from the coal cells within the subject pillar indicated pillar pressure to be 3,550 and 4,900 psig. Drilling of this low-stress pillar produced only the expected cutting volume of 2 gal per steel advance (40 in) and did not significantly change the pillar pressure or induce roof-to-floor convergence in the adjacent rooms.

In surveys 9 and 10, under high-stress conditions, two side-by-side pillars were drilled, hole 9 followed by hole 10, prior to the second cut of pillar splitting (fig. 40). Coal cells located two pillar rows outby the test site displayed maximum raw pressures of approximately 13,000 psig before and after the experiment. The first 10 ft of both holes displayed similar behavior to the low-stress test, expected cuttings volume for a 3.9-in-diam bit and no induced roof-to-floor convergence (fig. 41). However, drilling in the 10- to 23-ft-deep zone of the high-stress pillars produced as much as 180 times the expected cuttings volume and 0.024 in of roof-to-floor convergence per steel advance (40 in).

Both the cumulative cuttings volume and roof-to-floor convergence (fig. 41) data show that pillar 9 was under higher stress conditions than pillar 10. Possibly because pillar 9 was slightly smaller than pillar 10. Further analysis of cuttings volume and roof-to-floor convergence data per steel advance shows that a linear relationship, very similar to that displayed by the cumulative results for all 11 tests (fig. 38), exists between the two data sets. Only one point falls outside the 95-pct-confidence interval (fig. 42) for the equation $y = 0.006(x) + 0.96$, with an R-square value of 0.88, using the units gallons for the x axis and 0.001 in for the y axis.

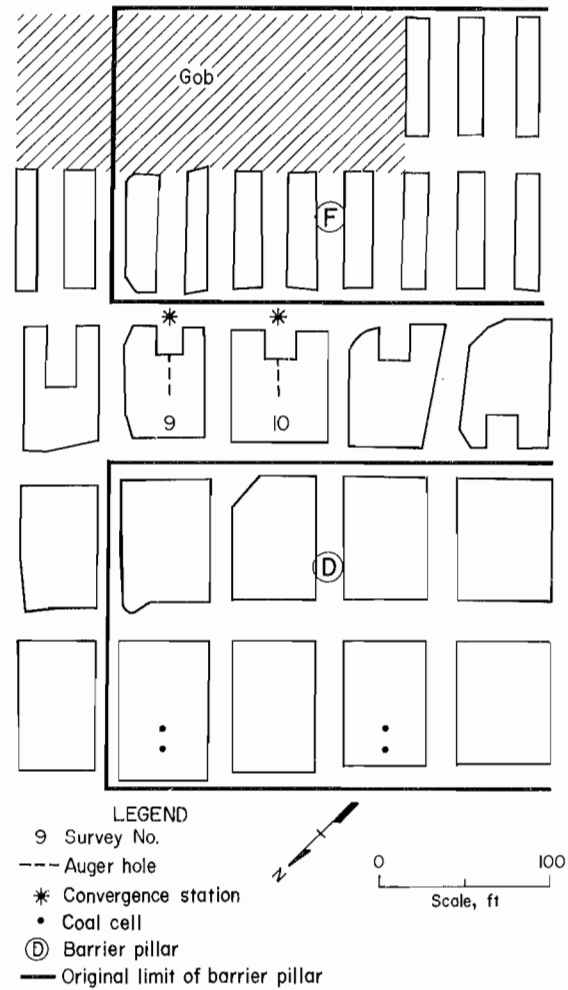


Figure 40.—Plan view of auger drilling surveys 9 and 10.

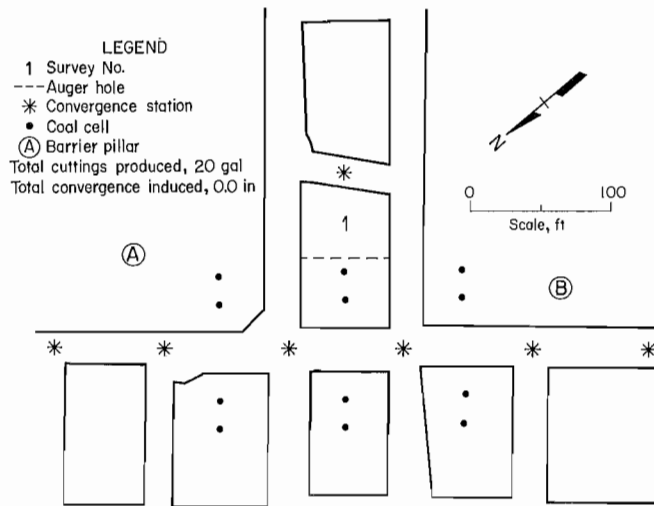


Figure 39.—Plan view of auger drilling survey 1.

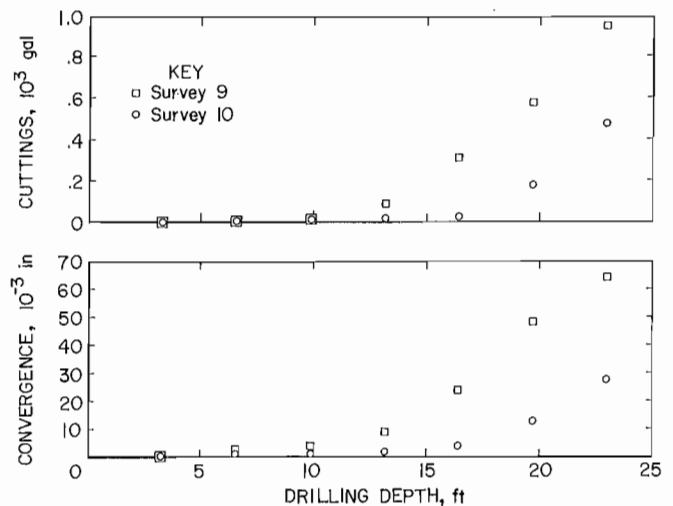


Figure 41.—Cumulative cuttings volume and cumulative roof-to-floor convergence versus drilling depth for auger drilling surveys 9 and 10.

Mining of the high-stress auger drilled cuts was observed. During the first 10 ft of advance by the continuous miner, the holes remained cylindrical. This mirrors the coal extensometer delineated yielded perimeter, confinement zone. In the 10- to 20-ft-deep drilling depth, the holes became a V-shaped cavity, forming a fissure as wide as 30 in at the top of the coal pillar (fig. 43). It is postulated that the vertical stress in the pillar had been greatly reduced. If the stress field had not been reduced, the void would have been closed. Only cylindrical holes were found in the low-stress application. Thus, high pillar pressure levels are necessary if the auger drilling for stress reduction is to be effective.

Auger drilling surveys 4 (fig. 44), 5 (fig. 45), and 6 (fig. 46) were in the barrier pillar (G), in which a lost-time bump accident occurred. Detailed convergence surveys during mining were conducted in the cuts, taken along the drilling direction, directly after auger drilling (fig. 33). A correlation between the average convergence per 5 st mined and the total convergence induced by auger drilling is evident. Average roof-to-floor convergence per 5 st mined of 0.001, 0.007, and 0.11 in coincide with 0.008,

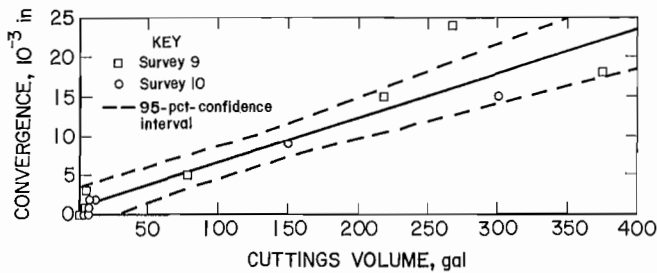


Figure 42.—Roof-to-floor convergence versus cuttings volume produced per steel advance (surveys 9 and 10).

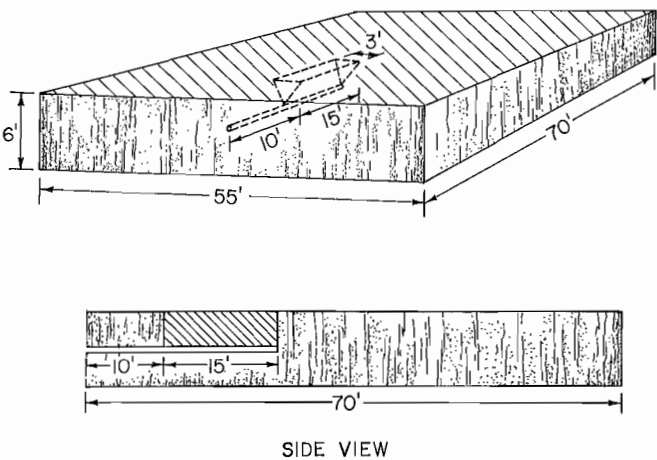


Figure 43.—Illustration of effect of auger drilling in high-stress pillars.

0.029, and 0.046 in of roof-to-floor convergence induced by auger drilling prior to the mining of the subject cuts. The auger drilling of the bump accident cut, survey 5, was deemed to be effective by the 870 gal of cuttings and 0.046 in roof-to-floor convergence responses. However, it was insufficient to prevent the bump, which caused an instantaneous roof-to-floor convergence of 1.001 in. This illustrates the extreme bump hazard associated with the splitting of barrier pillars adjacent to gob areas.

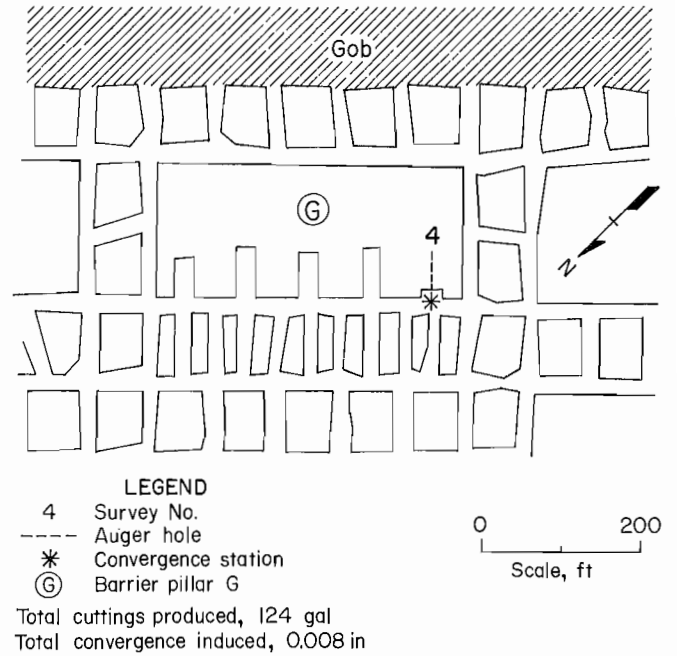


Figure 44.—Plan view of auger drilling survey 4.

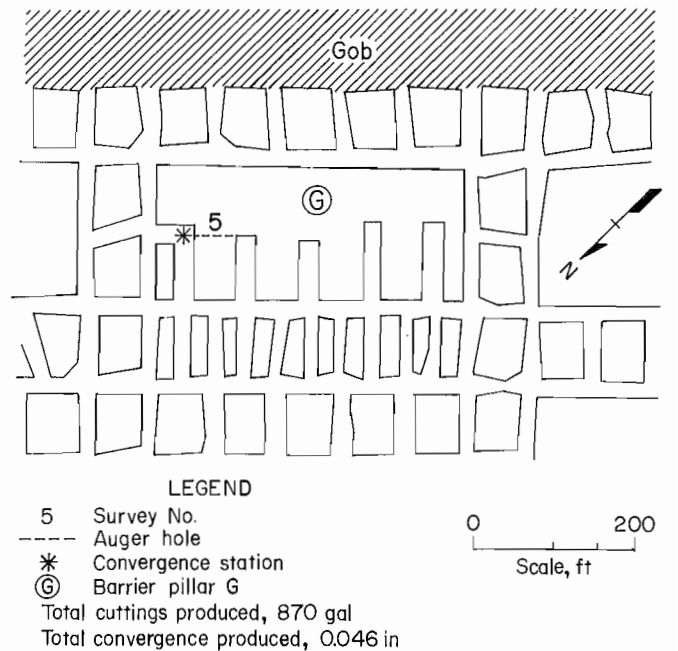


Figure 45.—Plan view of auger drilling survey 5.

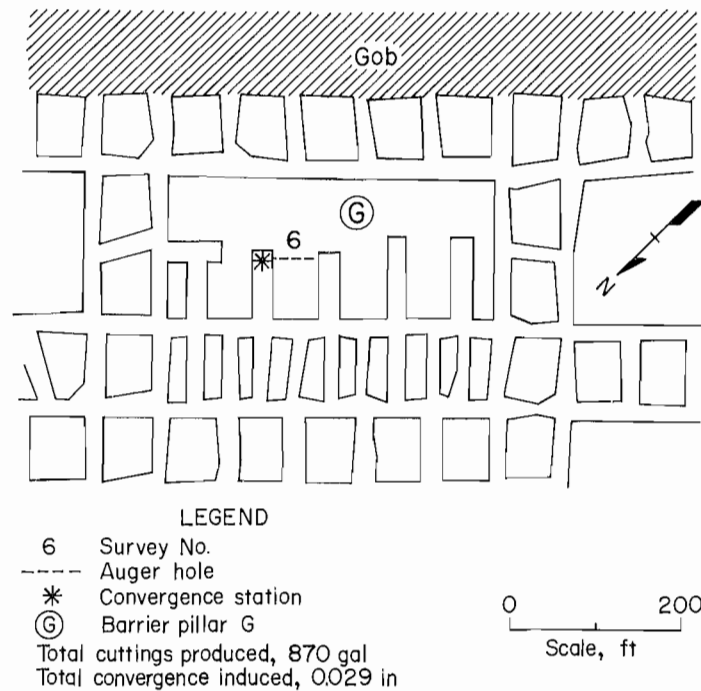


Figure 46.—Plan view of auger drilling survey 6.

SUMMARY AND CONCLUSIONS

The pillar splitting, retreat mining system practiced at the Olga Mine proved to be effective in redistributing abutment zone loads away from the pillar line. Large pillar pressure increases and roof-to-floor convergence were measured up to six chain pillar rows outby the newly formed gob during chain pillar retreat mining. This is in contrast to the localized effect of barrier splitting, advance mining. While the bump hazard is more extreme during the mining of highly stressed barriers, it includes a much wider area during chain pillar retreat.

Horizontal stress was not a contributing factor in causing bumps at the Olga Mine. The average horizontal principal stresses at the Olga Mine are 3,000 psi at N 60° E and 2,000 psi at N 30° W. The magnitude and direction of these stresses are close to the average measured at other southern West Virginia coal mines, which are not prone to mountain bumps.

Roof-to-floor convergence monitoring proved to be a very valuable tool in evaluating the pillar splitting mining method and localized destressing techniques at the Olga Mine. Consistent indications of pillar loading and stress redistribution resulted, because both the competent roof and floor rocks acted as large thick plates during the entire mining period, causing the soft coalbed to yield during chain pillar retreat mining.

A characteristic roof-to-floor convergence was associated with each type of continuous miner cut. Barrier splitting, advance mining induced little roof-to-floor convergence indicating the barriers and the resulting chain pillars were resistant to yielding and thus accumulated strain energy. Maximum strain energy storage in chain pillars appears to have occurred just prior to the first of four split cuts. At that point, a 15-ft-wide failed perimeter of the 55- by 70-ft pillars confined the core permitting the chain pillar to support tremendous pressures. Splitting the chain pillars into 17.5- by 70-ft wings practically removed the confinement load, allowing structural failure of the entire chain pillar to occur after the third pillar split cut.

A roof-to-floor convergence response to all volley firings in the shot fire experiments was noted. This indicates softening of the destressed pillars resulting in a reduction of their strain energy storage. The effectiveness of shot firing increases with the amount of explosives employed. The effect of pillar geometry, hole spacing, and simultaneous treatment of multiple pillars merits further study.

A direct linear relationship exists between induced roof-to-floor convergence and cuttings volume produced by auger drilling for pillar destressing. Both data sets indicate that high pillar pressure levels (greater than 10,000 psi) are necessary if the auger drilling for stress reduction is to

be effective. Destressing was most effective directly in advance of the second and third chain pillar split cuts, during chain pillar retreat mining. The effects of bit size and

drilling multiple holes in a single pillar warrant further study.

REFERENCES

- Holland, C. T., and E. Thomas. Coal Mine Bumps: Some Aspects of Occurrence, Cause, and Control. BuMines B 535, 1954, 37 pp.
- Khair, A. W., A. L. Grayson, and N. P. Reddy. The Effect of Immediate Strata on Pillar Behavior in Retreat Pillaring—A Case Study. Paper in Proceedings of the Fifth Conference on Ground Control in Mining, ed. by A. Khair and S. Peng. WV Univ., 1986, pp. 257-277.
- Bieniawski, Z. T. Strata Control. Wiley, 1987, pp. 135-147.
- King, R. L., and B. T. Brady. Mountain Bump Research at the Bureau of Mines. Paper in Proceedings of the 18th Annual Institute of Coal Mining Health, Safety, and Research, Blacksburg, VA, Aug. 25-27, 1987. VA Polytechnic Inst. and State Univ. 1987, pp. 159-165.
- Condon, J. L., and R. D. Munson. Microseismic Monitoring of Mountain Bumps and Bounces: A Case Study. Paper in Proceedings of the Sixth International Conference on Ground Control in Mining, Morgantown, WV, Univ. June 9-11, 1987. WV Univ., 1987, pp. 1-9.
- Campoli, A. A., C. A. Kertis, and C. A. Goode. Coal Mine Bumps: Five Case Studies in the Eastern United States. BuMines IC 9149, 1987, 34 pp.
- Iannacchione, A. T., A. A. Campoli, and D. C. Oyler. Fundamental Studies of Coal Mine Bumps in the Eastern Portion of the United States. Paper in Rock Mechanics, ed. by I. Farmer, J. J. K. Daemoan, C. S. Desai, C. E. Glass, and S. P. Newman. A. A. Balkema, 1987, pp. 1063-1072.
- Hennen, R. V. Wyoming and McDowell Counties. WV Geol. Surv. County Rep., 1915, 783 pp.
- Deere, D. U., J. R. Dunn, R. H. Fickies, and R. J. Proctor. Geologic Logging and Sampling of Rock Core for Engineering Purposes, Appendix K. WV Geol. Surv., 1977, 15 pp.
- Newman, D. A. The Design of Coal Mine Roof Support and Yielding Pillars for Longwall Mining in the Appalachian Coalfields. Ph.D. Thesis, PA State Univ., University Park, PA, 1985, 392 pp.
- Blankenship, C., and A. T. Castanon. Multiple Fatal Bump Accident (Outburst). MSHA, Arlington, VA, 1983, 17 pp.
- Hayduk, M. (retired chief engineer, U.S. Steel Corp.). Private communication, 1985; available upon request from A. A. Campoli, BuMines, Pittsburgh, PA.
- Bauer, E. R., G. J. Chekan, and J. H. Hill III. A Borehole Instrument for Measuring Mining Induced Pressure Changes in Underground Coal Mines. Paper in 26th U.S. Symposium on Rock Mechanics. A. A. Balkema, v. 2, 1985, pp. 1075-1084.
- Bieniawski, Z. T. Rock Mechanics Design in Mining and Tunneling. A. A. Balkema, 1984, pp. 191-192.
- Oyler, D. C., A. A. Campoli, and F. E. Chase. Factors in Influencing the Occurrence of Coal Pillar Bumps at the 9-Right Section of the Olga Mine. Paper in Proceedings of the Sixth International Conference on Ground Control in Mining, Morgantown, WV, June 9-11, 1987. WV Univ., 1987, pp. 10-17.
- Agapito, J. F. T., S. J. Mitchell, M. P. Hardy, and W. N. Hoskins. Determination of In Situ Horizontal Rock Stress on Both a Mine-Wide and District-Wide Basis (contract J0285020, Tosco Res., Inc.). BuMines OFR 143-80, 1980, 175 pp.; NTIS PB 81-139735.
- Worotnicki, G., and R. Walton. Triaxial "Hollow Inclusion" Gauges for Determination of Rock Stresses In Situ. Paper in the Symposium on Investigation of Stress in Rock. Inst. Eng., Australia Natl. Conf. Publ. No. 76/4, 1976, pp. 1-8.
- Campoli, A. A., M. Trevits, and G. M. Molinda. Coal and Gas Outbursts: Prediction and Prevention. Coal Min., v. 22, No. 12, 1985, pp. 42-44, 47.
- Campoli, A. A. Evaluating Coal Mine Bump Control Techniques Through Convergence Monitoring. Coal Min., v. 24, No. 7, 1987, pp. 42-46.
- Paul, K. Further Development of Methods for Predicting and Preventing Gas Outbursts. Glukauf (Engl. transl.), July 9, 1981, pp. 334-337.
- Davies, A. W. Available Defenses Against Outbursts in the United Kingdom in 1980. Paper in the Occurrence, Prediction, and Control of Outbursts in Coal Mines Symposium. Australian I. M. M. Southern Queensland Branch, Sept. 1980, pp. 203-215.
- Obert, L. In Situ Determination of Stress in Rock. Min. Eng. (Littleton, CO), v. 14, No. 8, 1962, pp. 51-58.
- Hooker, V. E., and C. F. Johnson. Near-Surface Horizontal Stresses Including the Effects of Rock Anisotropy. BuMines RI 7224, 1969, 29 pp.
- Bickel, D. L. Overcoring Equipment and Techniques Used in Rock Stress Determination (An Update of IC 8618). BuMines IC 9013, 1985, 27 pp.

APPENDIX.—BOREHOLE DEFORMATION GAUGE PROCEDURES AND RESULTS

The Bureau of Mines borehole deformation gauge was used in vertical core holes drilled into the roof to measure the horizontal components of in situ stress. Boreholes 5 and 6 were drilled in the 9 Right section of the Olga Mine (figure 6, main text) and borehole 15 was drilled in the 8 Right section located 2 miles from the 9 Right section (fig. 3). The stresses were computed from the field data using both the isotropic equations described by Obert (22)¹ and by the anisotropic method described by Hooker and Johnson (23).

The isotropic method requires a single estimate of Poisson's ratio and of the modulus of elasticity, and assumes an isotropic material. The anisotropic method requires Poisson's ratio and modulus of elasticity values for the axial direction and two orthogonal axes perpendicular to the axis of the borehole. The anisotropic method also requires a value of the axial stress. An axial stress value based on 1.1 psi times the overburden depth (an estimate of the lithologic pressure) was used to estimate the axial stress in the anisotropic computations of table A-1.

Both of the orthogonal horizontal modulus of elasticity values were available for cores that were biaxially tested.

Values from tested cores were used for those cores that had not been biaxially tested. The axial modulus of elasticity was estimated for all of the cores from the average value obtained from uniaxial tests of three samples obtained in core holes in the 9 Right study area. The same samples were used to generate the only available estimate of Poisson's ratio. Estimates of the horizontal stress are only slightly changed by taking the axial stress into account and are even less affected by corrections made for the anisotropic properties of the rock.

Four stress measurements were made in hole 5 at depths from 5.8 to 12.9 ft (depths measured from the top of the coalbed upward), three measurements were taken in hole 6 at depths from 3.7 to 6.3 ft, and 6 measurements were taken in hole 15 at depths from 2.3 to 11.8 ft. The results are summarized in table A-1. Most of the cores obtained were also tested in the biaxial simulator (24) to determine the magnitude and direction of the maximum and minimum values of the modulus of elasticity. These values are also included in table A-1. No biaxial test was conducted on core 6-G because the core broke at a thin clay layer at the beginning of the test operation. The core broke at a pressure of 600 psi.

¹Italic numbers in parentheses refer to items in the list of references preceding this appendix.

Table A-1.—Anisotropic and isotropic stress computation of borehole deformation gauge results

(Poisson's ratio, 0.26; E_{33} , 5.16×10^6 psi; both from laboratory testing of rock samples)

| Hole and test | Test depth, ft | Strain readings, ¹ microstrain | | | Young's modulus, 10 ⁶ psi | | | Principal compressive stresses, psi | | | | P direction ² | |
|--------------------------|----------------|---|----------------|----------------|--------------------------------------|-----------------|-----------------------------|-------------------------------------|-------|-----------|-------|--------------------------|-----------|
| | | U ₁ ³ | U ₂ | U ₃ | E ₁₁ | E ₂₂ | A _v ⁴ | Anisotropic | | Isotropic | | Anisotropic | Isotropic |
| | | | | | | | | P | Q | P | Q | | |
| 5-B | 5.8 | 1,630 | 1,550 | 3,010 | 2.86 | 3.33 | 3.10 | 2,800 | 1,600 | 2,800 | 1,800 | N 52° E | N 54° E |
| 5-C ⁵ | 7.8 | 1,667 | 1,811 | 3,007 | 2.86 | 3.33 | 3.10 | 2,800 | 1,800 | 2,900 | 1,900 | N 56° E | N 58° E |
| 5-D ⁵ | 9.9 | 1,626 | 2,311 | 2,812 | 2.86 | 3.33 | 3.10 | 2,800 | 2,000 | 2,900 | 2,100 | N 67° E | N 73° E |
| 5-E ⁶ | 12.9 | 1,855 | 1,873 | 2,870 | 3.33 | 3.85 | 3.59 | 3,000 | 2,300 | 3,300 | 2,400 | N 62° E | N 55° E |
| 5-E ⁶ | 12.9 | 1,855 | 1,873 | 2,870 | 3.45 | 4.35 | 3.96 | 3,500 | 2,300 | 3,500 | 2,600 | N 53° E | N 55° E |
| 6-D | 3.7 | 763 | 196 | 1,562 | 5.56 | 6.25 | 5.90 | 2,500 | 1,000 | 2,600 | 900 | N 42° E | N 43° E |
| 6-E | 4.5 | 2,609 | 3,067 | 1,463 | 1.82 | 3.57 | 2.69 | 2,300 | 1,700 | 2,700 | 1,800 | N 70° W | N 43° W |
| 6-G ⁵ | 6.3 | 1,253 | 1,669 | 1,959 | 2.86 | 3.33 | 3.10 | 2,000 | 1,500 | 2,000 | 1,600 | N 68° E | N 73° E |
| 15-B | 2.3 | 194 | 1,342 | 2,967 | 3.56 | 4.03 | 3.80 | 2,900 | 900 | 3,100 | 900 | N 66° E | N 67° E |
| 15-C | 3.8 | 925 | 2,391 | 2,914 | 2.25 | 2.78 | 2.52 | 2,300 | 1,300 | 2,400 | 1,300 | N 72° E | N 78° E |
| 15-D | 5.2 | 1,055 | 2,083 | 3,029 | 2.88 | 3.57 | 3.23 | 2,900 | 1,600 | 3,000 | 1,700 | N 66° E | N 71° E |
| 15-E | 6.6 | 816 | 1,476 | 2,437 | 3.38 | 3.80 | 3.59 | 2,500 | 1,300 | 2,600 | 1,400 | N 64° E | N 67° E |
| 15-F | 8.0 | 1,159 | 1,572 | 2,464 | 3.64 | 4.37 | 4.01 | 2,800 | 1,800 | 3,000 | 1,900 | N 61° E | N 64° E |
| 15-J | 11.8 | 2,661 | 2,232 | 618 | 2.31 | 2.64 | 2.48 | 2,000 | 1,000 | 2,200 | 1,100 | N 27° W | N 29° W |

¹All values are negative.

²Corrected for N 5° W magnetic declination.

³Magnetic north in all cases.

⁴Used in isotropic computations.

⁵No biaxial test, Young's modulus from 5-B used.

⁶2 biaxial tests run at 1,500 psi.

The measurements show a consistent northeast-southeast direction for the maximum horizontal secondary principal stress, with the exception of measurements 6-E and 15-J. Hole 6 was drilled in a roll area and the stresses determined by test 6-E may have been affected by this local geologic anomaly. However, no such conditions existed in the case of test 15-J and there is no obvious reason for the change in direction of the principal horizontal stresses. The stresses determined in tests 6-E and 15-J were assumed anomalous and have been dropped from the estimates of the mine-wide average stress. Based

upon 11 tests, the average horizontal secondary principal stress at the Olga Mine appears to be 2,700 psi (standard deviation 400 psi) at N 61° E (standard deviation 9°) and 1,600 psi (standard deviation 400 psi) at N 29° W. If measurements from the lower portions of the holes are discounted, assuming that those tests were affected by the presence of the mine opening, then the average horizontal principal stresses (based upon three measurements) are 3,000 psi (standard deviation 400 psi) at N 60° E (standard deviation 7°) and 2,000 psi (standard deviation 250 psi) at N 30° W.